

Inhomogeneous chemical evolution of the Galactic disk: evidence for sequential stellar enrichment?

L.B. van den Hoek¹ and T. de Jong^{1,2}

¹ Astronomical Institute 'Anton Pannekoek', Kruislaan 403, NL 1098 SJ Amsterdam, The Netherlands

² Space Research Organisation of the Netherlands, Sorbonnelaan 2, NL 3584 CA Utrecht, The Netherlands

Accepted 19/6/96

Abstract. We investigate the origin of the abundance variations observed among similarly aged F and G dwarfs in the local Galactic disk. We argue that orbital diffusion of stars in combination with radial abundance gradients is probably insufficient to explain these variations.

We show that episodic and local infall of metal-deficient gas can provide an adequate explanation for iron and oxygen variations as large as $\Delta[M/H] \sim 0.6$ dex among stars formed at a given age in the solar neighbourhood (SNBH). However, such models appear inconsistent with the observations because they: 1) result in current disk ISM abundances that are too high compared to the observations, 2) predict stellar abundance variations to increase with the lifetime of the disk, and 3) do not show substantial scatter in the $[Fe/H]$ vs. $[O/H]$ relation. Notwithstanding, our results do suggest that metal-deficient gas infall plays an important role in regulating the chemical evolution of the Galactic disk.

We demonstrate that sequential enrichment by successive stellar generations within individual gas clouds can account for substantial abundance variations as well. However, such models are inconsistent with the observations because they: 1) are unable to account for the full magnitude of the observed variations, in particular for $[Fe/H]$, 2) predict stellar abundance variations to decrease with the lifetime of the disk, and 3) result in current abundances far below the typical abundances observed in the local disk ISM.

We present arguments in support of *combined* infall of metal-deficient gas and sequential enrichment by successive stellar generations in the local Galactic disk ISM. We show that galactic chemical evolution models which take into account these processes simultaneously are consistent with both the observed abundance variations among similarly aged F and G dwarfs in the SNBH *and* the abundances observed in the local disk ISM. For reasonable choices of parameters, these models can reproduce

$\Delta[M/H]$ for individual elements $M = C, O, Fe, Mg, Al,$ and Si as well as the scatter observed in abundance-abundance relations like $[O/Fe]$. For the same models, the contribution of sequential stellar enrichment to the magnitude of the observed abundance variations can be as large as $\sim 50\%$.

We discuss the impact of sequential stellar enrichment and episodic infall of metal-deficient gas on the inhomogeneous chemical evolution of the Galactic disk.

Key words: Galaxy: chemical evolution, abundances, solar neighbourhood – ISM: abundances – Galaxies: ISM

1. Introduction

The chemical enrichment of the interstellar medium (ISM) by successive generations of stars is a key issue in understanding the chemical evolution of galaxies in general, and the formation history and abundance distributions of the stellar populations in our Galaxy in particular. Observational studies related to the heavy element enrichment of the local Galactic disk have long shown that stars of similar age exhibit large abundance variations (e.g. Mayor 1976; Twarog 1980a; Twarog & Wheeler 1982; Carlberg et al. 1985; Gilmore 1989; Klochkova et al. 1989; Schuster & Nissen 1989; Meusinger et al. 1991). Recently, Edvardsson et al. (1993a) presented accurate abundance data for nearly 200 F and G main-sequence dwarfs in the solar neighbourhood (SNBH). Their spectroscopic data, analysed with up-to-date input physics, confirms abundance variations as large as ~ 0.6 dex in $\Delta[M/H]$ (where $M=Fe,O,Mg,Al,Si$) among similarly aged stars. In contrast to previous understanding, these variations are much in excess of experimental uncertainties and demonstrate that the abundance spread for stars born at roughly the same galactocentric distance is similar in magnitude to

Send offprint requests to: L.B. van den Hoek (bobby@astro.uva.nl)

the overall increase in metallicity during the lifetime of the disk.

Additional support for the existence of large abundance inhomogeneities in the Galactic disk has been provided by studies of stars in open clusters (e.g. Nissen 1988; Boesgaard 1989; Lambert 1989; Garc a-Lopez et al. 1993; Friel & Janes 1993; Carraro & Chiosi 1994) and B stars in star forming regions in the SNBH (e.g. Gies & Lambert 1992; Cunha & Lambert 1992). These studies show that the concept of a well-defined tight age-metallicity relation (AMR) for the Galactic disk ISM is unfounded (Edmunds 1993) and that the chemical enrichment of the disk has been inhomogeneous on time scales as short as $\sim 10^8 - 10^9$ yr. Similar studies of objects in the Magellanic clouds (e.g. Cohen 1982; Da Costa 1991; Olsewski et al. 1991) and dwarf galaxies (Pilyugin 1992; Kunth et al. 1994; Thuan et al. 1995) suggest that inhomogeneous chemical evolution is a common phenomenon in nearby galaxies as well.

The origin of the abundance variations observed in the local Galactic disk is investigated in this paper. Clearly, large abundance variations in the ISM on time scales at least an order of magnitude shorter than the lifetime of the disk cannot be reproduced by simple galactic evolution models incorporating monotonously increasing age-metallicity relations (AMR). In the past few years, various ideas have been put forward as possible explanations for the intrinsic abundance variations among similarly aged stars:

- stellar orbital diffusion in combination with radial abundance gradients in the Galactic disk (e.g. Francois & Matteucci 1993; Wielen, Fuchs, & Dettbarn 1996);
- sequential enrichment by successive stellar generations (e.g. Edmunds 1975; Olive & Schramm 1982; Gilmore 1989; Gilmore & Wyse 1991; Cunha & Lambert 1992; Roy and Kunth 1995);
- local infall of metal-poor gas (e.g. Edvardsson et al. 1993a; Roy & Kunth 1995; Pilyugin & Edmunds 1995a);
- cloud motions in the ISM (Bateman & Larson 1993);
- inefficient mixing in the disk ISM: isolated chemical evolution of individual parcels of interstellar gas during considerable fractions of the lifetime of the disk (Lennon et al. 1990; Wilmes & K ppen 1995);
- major galaxy merger events resulting in multiple stellar populations in the Galactic disk (Strobel 1991; Pilyugin & Edmunds 1995b);
- chemical fractionization processes such as grain formation (e.g. Henning & G rtler 1986) and/or element diffusion (e.g. Bahcall & Pinsonneault 1995) so that measured abundances do not reflect initial stellar abundances.

As discussed by Edvardsson et al. (1993a) stellar orbital diffusion is probably inadequate as main explanation for the observed abundance variations. However, recently

Wielen et al. (1996) claimed that stars can be born at galactocentric distances very different from those derived using their present-day orbits. In this case, a major fraction of the observed abundance scatter could be due to stellar orbital diffusion. Since it appears unlikely that diffusion can explain the observed abundance variations for all stars in the Edvardsson et al. sample (see below) as well as those observed among young stars (e.g. present in star forming regions) other processes are probably important as well.

Based on the assumption of short mixing time scales of $\sim 10^7$ yr in the local disk ISM, we argue that the underlying physical mechanisms causing the observed abundance inhomogeneities and those initiating star formation in the disk ISM are the same. No observational support exists for chemical fractionization in low mass F and G main-sequence stars. Therefore, the scatter in stellar metallicities probably reflects the original inhomogeneities in the interstellar gas (e.g. Gilmore 1989). We here restrict ourselves mainly to the processes of sequential stellar enrichment and episodic infall of gas onto the Galactic disk as possible explanation for the observed stellar abundance variations. Since these processes are observed to operate simultaneously in the SNBH (see below), it is important to investigate their combined effect on the chemical evolution of the Galactic disk.

The process of star formation initiated by stars formed during a preceding star formation event nearby, is known as sequential star formation. Support for sequential star formation in the SNBH is provided by observations of spatially separated subgroups of OB stars that appear aligned in a sequence of ages in many OB associations (e.g. Blaauw 1991) and by observations of stars forming at the interfaces of HII regions and their surrounding molecular clouds (e.g. Genzel & Stutzki 1989; Pismis 1990; Goldsmith 1995). Sequential star formation may be induced by the blast waves of nearby supernova explosions compressing the ambient ISM (e.g. Ogelman & Maran 1976) and/or by propagating ionization and shock fronts from an OB association causing the gravitational collapse of a nearby molecular cloud (e.g. Elmegreen & Lada 1977). In either case, efficient self-enrichment through mixing of enriched material by successive generations of massive stars is expected.

On the other hand, stellar abundance variations can be attributed to infall of relatively unprocessed gas and star formation within the accreted material before efficient mixing wipes out any local chemical inhomogeneities (e.g. Edvardsson et al. 1993a; Pilyugin & Edmunds 1995a). Observational support for star formation in the SNBH initiated by infall of high velocity clouds, has recently been presented by L pine & Duvert (1994). These authors claim that episodic gas infall is a dominant process in the local disk ISM and is associated with all prominent star forming molecular clouds seen near the Sun (see Sect. 5.2). Furthermore, ongoing gas infall has been emphasized by models of dissipative protogalactic collapse (Larson 1969,

1976) and on the basis of time scale arguments of gas consumption in the local disk (Larson et al. 1980; Kennicutt 1983).

In this paper, we present a chemical evolution model for a star forming gas cloud which incorporates stellar enrichment and mixing processes (including infall) and which allows for temporal and/or spatial inhomogeneities in the ISM. This study differs from previous work (e.g. Pilyugin & Edmunds 1995a) in that we investigate in detail the combined effect of metal deficient gas infall and sequential stellar enrichment by successive stellar generations on the chemical evolution of multiple gas clouds in the Galactic disk. In particular, each gas cloud is allowed to follow its individual star formation, mixing, and infall history, as is suggested by the observations. With this model, we fit the stellar abundance variations and current local ISM abundances of C, O, Fe, Mg, Al, and Si observed in the SNBH, the present gas-to-total mass-ratio, and actual star formation and supernova rates. We note that previous investigations were restricted to abundance variations in oxygen and iron only.

We will show that models taking into account the above processes simultaneously are in good agreement with the observations and provide an adequate explanation for the stellar abundance variations with respect to the mean abundances observed in the local disk. Furthermore, we will argue that the contribution of sequential stellar enrichment to the magnitude of the observed stellar abundance variations can be as large as $\sim 50\%$, i.e. much larger than suggested by previous investigations (e.g. Pilyugin & Edmunds 1995a; Wilmes and Köppen 1995). Corresponding theoretical age and abundance-distributions related to the G-dwarf problem will be discussed in a separate paper.

The paper is organized as follows. In Sect. 2, we briefly review observations related to the inhomogeneous heavy element enrichment of the local Galactic disk ISM. In Sect. 3, we describe characteristics of the inhomogeneous chemical evolution model proposed for the Galactic disk (model equations and details are given in the Appendix to the electronic version of this paper). In Sect. 4, we present model results for episodic infall of metal-deficient gas and sequential stellar enrichment, and examine which of these mechanisms can account satisfactorily for the observations. In Sect. 5, we discuss these results in the more general context of the chemical evolution of the Galactic disk and adduce both observational arguments in support of sequential star formation and metal deficient gas infall in the local disk ISM.

2. Inhomogeneous chemical evolution of the local Galactic disk: observations

2.1. Main-sequence F and G dwarfs

We concentrate on the abundance data of nearly 200 main-sequence field F and G dwarfs with actual distances $\lesssim 70$ pc from the Sun as recently presented by Edvardsson et al. (1993a; hereafter EDV). This sample provides the largest sample of stars available to date for studies related to the chemical evolution of the local disk. Fig. 1 displays all F and G dwarfs for which both $[O/H]$ and $[Fe/H]$ abundance-ratios have been determined by EDV.

Large abundance variations of ~ 0.9 dex in $[Fe/H]$ and ~ 0.7 dex in $[O/H]$ among stars of a given age are seen to be present (abundance variations in e.g. Mg, Al, and Si resemble those in $[Fe/H]$). At intermediate stellar ages, these variations are no doubt significant since typical observational errors are ~ 0.1 dex both in $[M/H]$ and $\log(\text{Age})$ (see EDV). At ages in excess of ~ 15 Gyr and less than ~ 2 Gyr, the data probably are undersampled (see EDV). Note that the sample is biased against old, high-metallicity stars through the minimum T_{eff} limit assumed by EDV.

The observed spread in $[Fe/H]$ is tightly correlated with that in $[O/H]$. This suggests that different nucleosynthesis sites, which contribute different elements to the initial abundances in stars, mix their products together well. Furthermore, this suggests that stellar abundance variations for different elements are due to the same process. Current observations support the idea that the magnitude of the stellar abundance variations has remained constant over the lifetime of the disk (see also Mayor 1976; Twarog 1980a; Meusinger et al. 1991; Carraro & Chiosi 1994). In the following, we will assume that these abundance variations are randomly distributed within the metallicity range observed at a given stellar age. This is particularly important when considering possible explanations for the observed stellar abundance variations in detail (see Sect. 4; cf. Wielen et al. 1996).

Ages, abundances, and kinematical properties of the dwarfs belonging to the EDV sample are consistent with earlier investigations (e.g. Twarog 1980a; Carlberg et al. 1985; Meusinger et al. 1991). An extensive discussion of the possible sources of errors in the abundance and age analysis as well as several consistency checks can be found in Edvardsson et al. (1993a,b). Errors due to data reduction uncertainties are estimated to lead to errors of at most 0.05 to 0.1 dex in abundance ratios $[M/Fe]$ as well as in $[Fe/H]$ (see EDV). These errors are not expected to vary in a systematic manner with the derived stellar abundances and corresponding corrections will probably not reduce the observed variations. Edvardsson et al. estimated errors in relative ages of $\sim 25\%$ for stars with similar abundances (absolute errors may be considerably larger). Thus, ages of stars as old as the Sun are estimated to be accurate within $\sim 1-2$ Gyr. We conclude that errors in the abundances and ages of the sample stars are unlikely

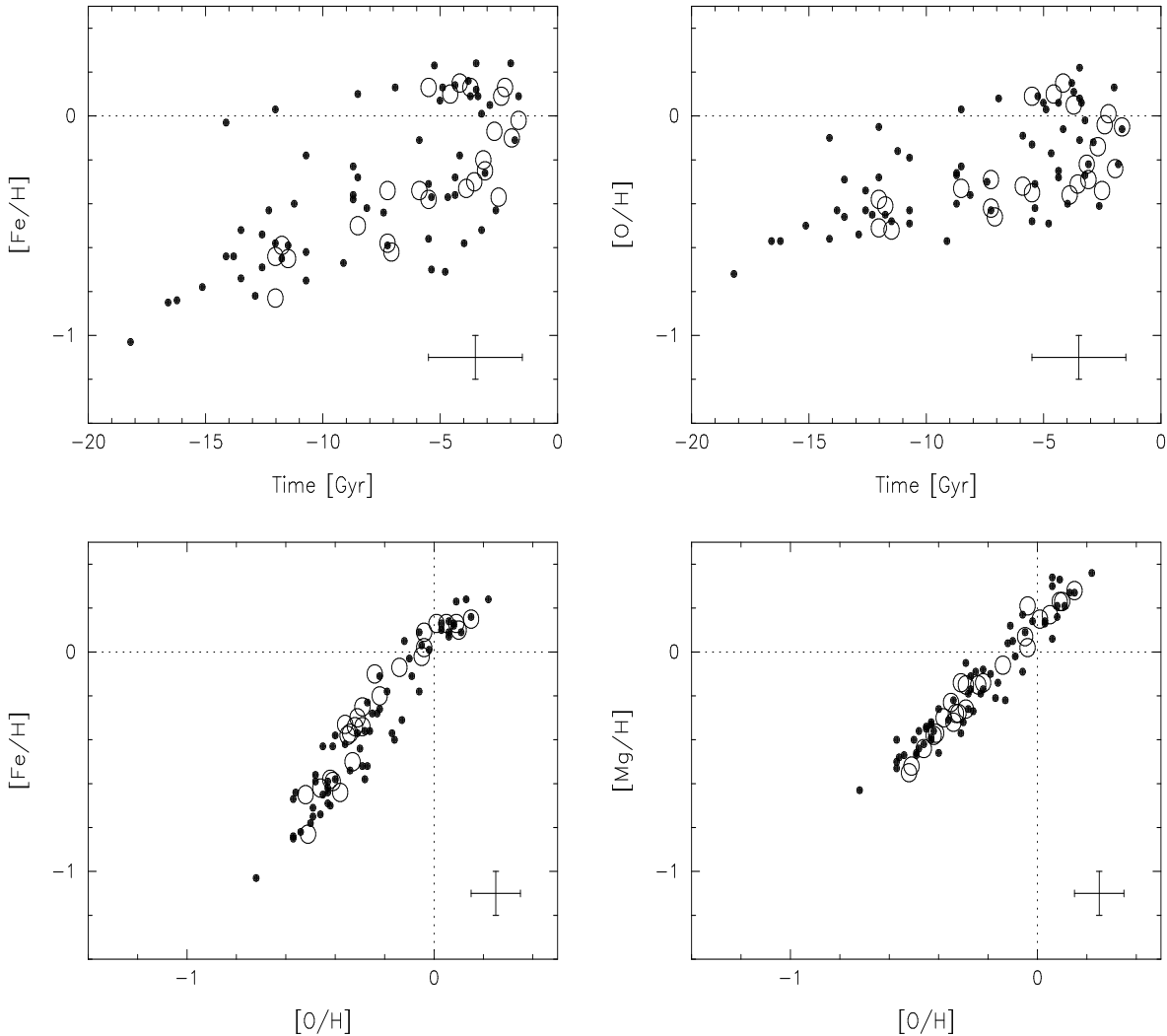


Fig. 1. Observed iron, oxygen, and magnesium abundance ratios for main-sequence F and G dwarfs in the solar neighbourhood (data from Edvardsson et al. 1993a). Open circles represent stars with mean stellar galactocentric distances at birth within 0.5 kpc from the Sun ($R_{\odot} = 8.4$ kpc). Full dots indicate stars with average distances within ~ 2 kpc from the Sun. Typical errors are indicated at the bottom right of each panel. Note that the abundances of the most metal-poor disk stars included in this sample resemble those of metal-rich halo dwarfs and giants (e.g. Bessell et al. 1991; Gratton & Snenen 1991; Nissen et al. 1994). We assumed solar abundance ratios by number of $^{10} \log (\text{O}/\text{H})_{\odot} = -3.13$, $^{10} \log (\text{Fe}/\text{H})_{\odot} = -4.51$, and $^{10} \log (\text{Mg}/\text{H})_{\odot} = -4.42$ and a hydrogen mass fraction in the Sun of 0.68 (see Anders & Grevesse 1989; Grevesse & Noels 1993). *Top panels:* Distributions of [Fe/H] (left) and [O/H] abundance ratios vs. galactic age. *Bottom panels:* [Fe/H] vs. [O/H] (left) and [Mg/H] vs. [O/H]

to account for the observed abundance variations, at least for stars with intermediate ages of ~ 5 Gyr.

Knowledge of the formation sites of the sample stars is important to decide whether or not orbital diffusion in combination with radial abundance gradients in the Galactic disk can provide an adequate explanation for the observed abundance variations. Galactocentric distances of the sample stars *at birth* were obtained using stellar orbits reconstructed from their *present-day* galactocentric

distances, proper motions, and radial velocities, and using both theoretical and empirical models for the Galactic potential as discussed by EDV. Accordingly, nearly 85% of the sample stars were found to have mean galactocentric distances R_m at birth within 1 kpc from the Sun (assuming $R_{\odot} \sim 8.4$ kpc at present). However, predictions of the diffusion of stellar orbits in space, based on the observed relation between velocity dispersion and age for nearby stars, suggest that many stars may have been formed at

galactocentric distances as large as ~ 4 kpc from where they are nowadays observed in the SNBH (Wielen et al. 1996). In either case, these nearby stars trace the evolution of the Galactic disk ISM over a much wider range in galactocentric distance than they are observed.

As an independent test to examine whether stellar orbital diffusion can be the main cause for the observed abundance variations, we translated stellar abundance deviations $\Delta[\text{M}/\text{H}]$ from the mean abundances of similar aged stars born at $\sim R_\odot$ into galactocentric distance differences $R_m - R_\odot$. This was done independently for $[\text{Fe}/\text{H}]$ and $[\text{O}/\text{H}]$ abundance ratios assuming present-day local radial abundance gradients of -0.07 ± 0.015 dex kpc^{-1} in $[\text{O}/\text{H}]$ (e.g. Shaver et al. 1983; Grenon 1987; see also Wilson & Matteucci 1992) and -0.1 dex kpc^{-1} in $[\text{Fe}/\text{H}]$ (see e.g. EDV). Clearly, distances R_m based on oxygen and iron abundances are expected to be similar (e.g. $\Delta R_m^{\text{O,Fe}} \lesssim 1$ kpc) when orbital diffusion is important for the observed stellar abundance variations.

In this manner, we find that $\Delta R_m^{\text{O,Fe}} \gtrsim 1$ kpc for 47 stars in the EDV sample (i.e. $\sim 56\%$). Similarly, we find $\Delta R_m^{\text{O,Fe}} \gtrsim 2, 3,$ and 4 kpc, for $\sim 31, 14,$ and 8% of the sample stars, respectively. We note that the derived values of $\Delta R_m^{\text{O,Fe}}$ are insensitive to the stellar age but depend on the assumed radial abundance gradients as well as on the mean $[\text{M}/\text{H}]$ vs. age relations adopted for stars born at R_\odot . Although a detailed investigation of the uncertainties involved is beyond the scope of this paper (e.g. the variation of abundance gradients with disk age; cf. Grenon 1987), we estimate that $\Delta R_m^{\text{O,Fe}} \lesssim 0.8$ (1.5) kpc for *typical* errors of 0.05 (0.1) dex in both $[\text{Fe}/\text{H}]$ and $[\text{O}/\text{H}]$ for most of the sample star (assuming a gaussian error distribution). This suggests that a substantial part of the observed abundance variations is difficult to explain by stellar orbital diffusion only.

Also, Edvardsson et al. argued that the magnitude of the observed variations will reduce to $\Delta[\text{M}/\text{H}] \sim 0.3$ dex if one accounts properly for systematic errors and possible effects of stellar orbital diffusion. However, a reduction of the abundance spread among field dwarfs to $\Delta[\text{Fe}/\text{H}] \sim 0.3$ dex seems contradicted by the observed variations of $\Delta[\text{Fe}/\text{H}] \sim 0.5 \pm 0.1$ dex among similarly aged open clusters *after* correcting for radial abundance gradients across the Galactic plane (Carraro & Chiosi 1994). Apart from this, such a reduction appears inconsistent with the observed abundance spread of $[\text{O}/\text{H}] \gtrsim 0.4$ dex among B stars at a given galactocentric radius between 7 and 16 kpc in the disk (Gehren et al. 1985; Kaufer et al. 1994) and with the large abundance variations of ~ 0.7 dex observed among young open clusters over a distance scale of only ~ 1 kpc at a galactocentric radius of ~ 13 kpc (Rolleston et al. 1994).

What fraction of the current disk stellar population actually formed in the Galactic halo depends on the detailed dynamical evolution of the disk which is not well known (e.g. Pagel & Tautvaisiene 1995). However, most

stars in the EDV sample have derived maximum distances from the Galactic plane at birth of $h_{\text{max}} < 0.5$ kpc. This largely excludes halo stars from the sample and further implies that abundance gradients perpendicular to the Galactic plane are inadequate as explanation for the observed abundance variations (e.g. Carney et al. 1990).

From these arguments, we conclude that orbital diffusion of stars from elsewhere in the Galactic disk is probably insufficient as explanation for the observed variations in $[\text{Fe}/\text{H}]$ and $[\text{O}/\text{H}]$ among F and G dwarfs in the SNBH. This conclusion is consistent with the finding that abundance variations for subsamples of stars restricted to be born within 1 and 0.5 kpc from the Sun, respectively, are similar to those for the complete sample (see EDV; cf. Fig. 1). Therefore, we believe that differential chemical evolution and mixing of interstellar gas must be an important cause for the large stellar abundance variations observed in the SNBH as well. The abundances of the Sun and of open clusters in the Galactic disk fit well into this picture, as is argued below.

2.2. Chemical evolution of the solar neighbourhood

Detailed comparison of abundances within local HII regions and the Sun have shown that oxygen (among other heavy elements) is underabundant in the HII regions by about 0.15–0.3 dex (e.g. Shaver et al. 1983; Peimbert 1987; Baldwin et al. 1991; Osterbrock, Tran & Veilleux 1992). Also, CNO-abundances of HII-regions and B main-sequence stars in the Orion nebula were found smaller than corresponding abundances in the Sun (Cunha & Lambert 1992; Gies & Lambert 1992). The remarkable result that the Sun is metal-rich by ~ 0.15 –0.2 dex in $[\text{O}/\text{H}]$ compared to its surroundings is also supported by observations of B stars in nearby associations and young clusters (Fitzsimmons et al. 1990), diffuse interstellar clouds (e.g. York et al. 1983), and disk planetary nebulae (de Freitas Pacheco 1993; Peimbert et al. 1993). Although abundance determinations in the SNBH may be biased towards regions associated with infall of metal-poor gas or suffer from heavy element depletion by dust, the existence of many metal-poor regions in the SNBH would be difficult to reconcile with efficient mixing in the local disk ISM (e.g. Roy & Kunth 1995).

The above observations are consistent with the Edvardsson et al. data which suggest that the Sun is metal-rich by 0.2–0.25 dex in $[\text{O}/\text{H}]$ and by 0.25–0.3 dex in $[\text{Fe}/\text{H}]$ compared to the mean abundances of stars which formed in the SNBH ~ 4.5 Gyr ago (cf. Fig. 1). These observations support the idea that the Sun is metal-rich for its age (see also Steigman 1993) and that abundance inhomogeneities in the local disk ISM did exist. The fact that the Sun is metal-rich by a factor of ~ 1.5 –2 compared to nearby regions currently experiencing star formation may be explained by self-enrichment of the gas cloud out of which the Sun was born (e.g. Gies & Lambert 1992; Pe-

imbert et al. 1993). Alternatively, orbital diffusion of the Sun may play an important role (Wielen et al. 1996). We will discuss arguments in support of the former possibility in Sect. 5.2.

2.3. Open clusters

Variations in $[\text{Fe}/\text{H}]$ among disk open clusters of a given age are known to be larger than any possible trend of $[\text{Fe}/\text{H}]$ with age (e.g. Nissen 1988; Boesgaard 1989; Garcia-Lopez et al. 1993; Friel and Janes 1993). Recently, abundance variations of $\sim 0.5 \pm 0.1$ dex in $[\text{Fe}/\text{H}]$ among clusters of a given age *after* correcting for the radial abundance gradient across the Galactic plane have been reported by Carraro & Chiosi (1994). The observed abundance variations among open clusters appear somewhat smaller (i.e. by $\sim 0.2\text{--}0.3$ dex in $[\text{Fe}/\text{H}]$) than those among field F and G dwarfs in the EDV sample. However, the magnitude of the observed variations suggests that the processes responsible for the abundance inhomogeneities among field stars in the SNBH and among open clusters widespread throughout the Galactic disk may well be the same.

The lack of a tight age-metallicity relationship for open clusters in the Galactic disk suggests that the chemical enrichment of the disk ISM has been inhomogeneous on time scales less than $\sim 10^8\text{--}10^9$ yr, consistent with the abundance variations observed for intermediate age F and G dwarfs discussed above.

3. Model characteristics and assumptions

In the previous section, we have argued that differential chemical evolution and mixing of interstellar gas probably provides the main explanation for the large abundance variations observed among similarly aged stars in the SNBH. In this case, abundance inhomogeneities in the global disk ISM may result from local mixing of metal-deficient material (e.g. infall) and/or local mixing of metal-enhanced material (e.g. stellar enrichment). When star formation is initiated within the mixed material before any abundance fluctuations are wiped out, these inhomogeneities can be recorded by long-living stars.

Efficient mixing by stellar winds and supernova explosions is generally accepted to occur within $\sim 10^7\text{--}10^8$ yr (e.g. Edmunds 1975; Ciotti et al. 1991; Roy & Kunth 1995). This suggests that the processes responsible for the onset of star formation and those causing substantial abundance inhomogeneities in the disk ISM are the same. We consider this as a strong argument in favour of sequential star formation and/or infall induced star formation as the main processes responsible for the observed abundance variations (ample observational support for the occurrence of these processes in the local disk ISM are briefly discussed in Sect. 5.2). Obviously, the quantitative effect of these processes on stellar abundance variations, *relative*

to the mean abundances in the local ISM, depends on the detailed chemical evolution of the disk ISM.

3.1. Model description

We present a model for the inhomogeneous chemical evolution of a star forming gas cloud. The basis for this model forms the individual star formation history and chemical evolution of multiple subclouds that mutually exchange interstellar material. We here restrict ourselves to a brief outline of the basic assumptions and model characteristics. A more detailed description of the equations and input physics used is given in the (Appendix to the) electronic version of this paper.

We start from a homogeneous gas cloud with total mass M_{cl} . At any time the cloud is subdivided into N_{sc1} star forming, active subclouds (with corresponding masses M_{sc1}^i) and a quiescent, inactive cloud part (with mass M_{qcl}) not experiencing star formation. Each subcloud is allowed to follow its individual star formation, infall, and mixing history. Infall of matter is considered by allowing episodic mixing of metal-deficient material to each subcloud separately.

The adopted set of processes that modify the distribution of gas and stars within a star forming region of a molecular cloud are illustrated in Fig. 2. Different subfigures refer to the following processes:

- (a) subcloud formation from the inactive cloud ISM (and/or from infalling material);
- (b) conversion of gas into stars (star formation at distinct subcloud cores);
- (c) ejection of material by stars to their immediate surroundings;
- (d) mixing of dispersed core material with subcloud after star formation event;
- (e) break up of entire subcloud, mixing with inactive cloud ISM, and induced star formation;
- (f) enrichment of subcloud by stars not formed within the subcloud.

In our model, the inhomogeneous chemical evolution of a star forming gas cloud, consisting of many subclouds, is determined by the combined effect of the above processes. During a time-interval Δt , these processes may occur simultaneously within each subcloud. In this manner, the initial abundances of a newly formed stellar generation are determined by: 1) the enrichment of the subcloud by preceding stellar generations, and 2) the mixing history of the subcloud with the ambient ISM.

In brief, the adopted evolution scenario is as follows. Subcloud formation (Fig. 2a) is assumed to occur either from the inactive cloud ISM and/or from infalling material (details related to the infall model will be given in Sect. 4.3). During the lifetime t_{ev} of the entire system, a total number of N_{sf} star formation events is assumed to occur. Each star formation event is assumed to take place in an

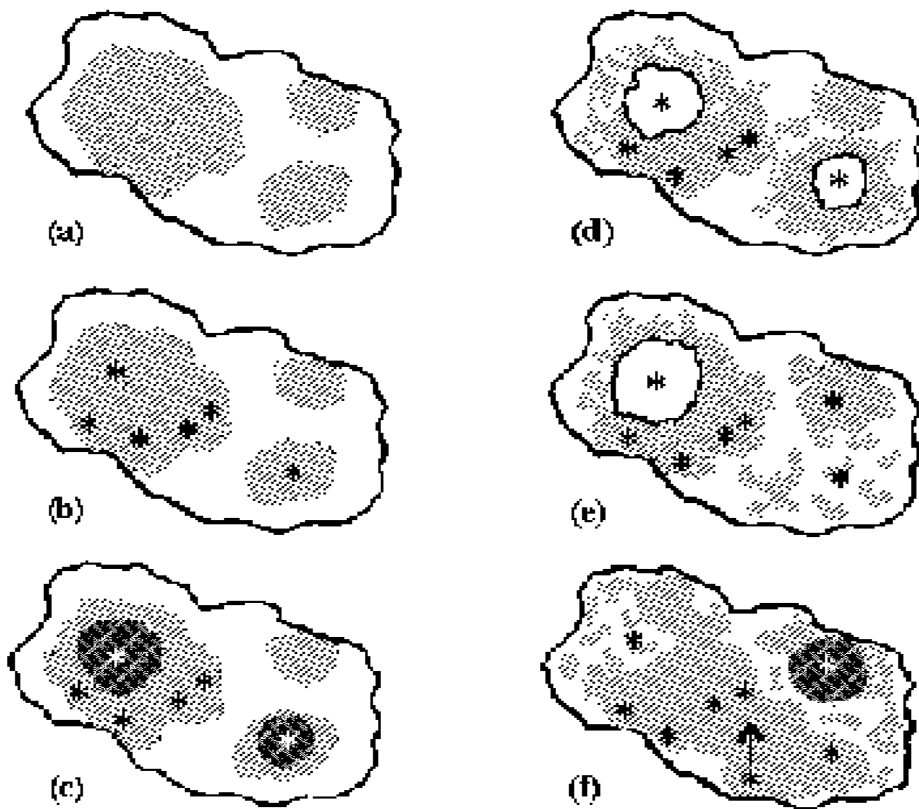


Fig. 2. Schematic model for the inhomogeneous chemical evolution of a star forming cloud: evolutionary sequence of star formation, enrichment and mixing processes. Shown is a star forming cloud region. Each of the processes indicated in this region may occur in other regions of the cloud as well. Symbols have the following meaning: **a** subclouds indicated by hatched areas, **b** star formation indicated by asterisks, **c** stellar enrichment shown as shaded areas enclosing white asterisks, **d** subcloud core dispersal indicated as blanked out area surrounding stars, **e** break up of entire subcloud and initiation of star formation in a nearby subcloud, **f** arrow indicates stars entering a subcloud from elsewhere. Each of the processes indicated may occur frequently during the cloud evolution time t_{ev} .

active subcloud (Fig. 2b). Each subcloud is allowed to experience numerous star formation events and/or to remain inactive during a substantial part of its lifetime. Consequently, each subcloud can be enriched by one or multiple star formation events dictating its chemical evolution (Fig. 2c). When the active subcloud *core* is dispersed by stellar winds and/or supernova shocks, part of the enriched matter is assumed to mix homogeneously with the surrounding subcloud material (Fig. 2d). The remaining part is assumed to mix homogeneously either to a nearby subcloud hosting the *next* star formation event or to the ambient inactive cloud part (Fig. 2e). No mass-exchange is assumed between the subcloud and the ambient inactive cloud ISM during the time interval in which two or more star formation events occur within the same subcloud. In addition, subcloud material may be enriched by stars formed outside the subcloud. In this case, stars from elsewhere in the inactive cloud occasionally enter the subcloud region and enrich the subcloud by means of their

ejecta (Fig. 2f). Stellar enrichment by old stellar generations is assumed to proceed continuously with time but is considered in detail only at specific evolution times corresponding to the occurrence of any of the discontinuous processes referred to in Fig. 2.

We define the subcloud core dispersal time Δt_{disp} as the time between onset of star formation within a subcloud core region and the complete dispersal of this region. This time interval constrains the mass of the most massive star that is able to enrich the subcloud core material before the core ultimately breaks up. Before dispersal of an *entire* subcloud, the subcloud will be enriched by the stellar populations it is hosting. After subcloud dispersal (i.e. after a typical mixing time scale Δt_{mix}), stars and gas belonging to the subcloud are assumed to mix instantaneously and homogeneously with the inactive cloud ISM. Subsequently, different cloud fragments may combine to form new subclouds wherein star formation occurs as soon as the critical conditions for star formation are

met. The mixing history of each subcloud determines the inhomogeneous chemical evolution of the inactive cloud part as well as that of nearby subclouds. For simplicity, we do not consider partial mixing of subcloud material to the inactive cloud.

3.2. Outline of model computations

We perform Monte-Carlo simulations of the inhomogeneous chemical evolution of a star forming gas cloud. The continuous process of formation and break up of subclouds and of the formation and dispersion of subcloud core regions associated with star formation, are followed as outlined in the previous section. During the evolution of the cloud, we keep track of the total mass contained in gas and stars as well as the stellar and interstellar abundances of H, He, C, O, Fe, Mg, Al, and Si, both within each subcloud and the inactive cloud part. No instantaneous recycling is assumed, i.e. metallicity dependent stellar lifetimes are taken into account.

3.3. Model input parameters

Model input parameters for the reference model are listed in Table 1. We distinguish parameters related to: 1) the entire cloud and inactive cloud part, 2) active subcloud regions, and 3) individual star formation events:

- *Cloud and inactive cloud part:* The initial cloud mass M_{cl} is treated as a mass scaling parameter (i.e. resulting abundances are not altered for different values of M_{cl}). We here adopted $M_{\text{cl}} = 5 \cdot 10^{10} M_{\odot}$ similar to that of the Galactic disk (e.g. Binney & Tremaine 1987). We assume a cloud evolution time $t_{\text{ev}} = 14$ Gyr. This is comparable to the age of the Galaxy as derived from the age of the oldest globular clusters, i.e. 14 ± 3 Gyr (e.g. Buonanno et al. 1989). In our model, the impact of processes causing stellar abundance variations does not depend on the specific age of the Galactic disk assumed.

We consider a total number of star formation events during the cloud evolution time of typically $N_{\text{sf}} = 100$. In practice, N_{sf} is limited only by the preferred model run time, i.e. 1-2 hours on a HP Apollo 715 machine. The total number of *subclouds* N_{scl} is determined by the number of star formation events within each subcloud. For the reference model, we assume a maximum number of star formation events within one subcloud $N_{\text{sf}}^{\text{max}} = 1$ so that $N_{\text{scl}} = N_{\text{sf}}$. Cloud initial abundances X_{qcl} are as given in Table 1. Initially, the cloud is considered homogeneous, metal-free, and void of stars.

- *Active subclouds:* In case of the reference model, we force subclouds to form at regular intervals of $t_{\text{ev}} / N_{\text{scl}} = 1.4 \cdot 10^8$ yr. We assume the subcloud mass M_{scl} directly proportional to the entire cloud gas-to-total mass-ratio μ at time of subcloud formation t_{scl} . This implies more massive subclouds to form at relatively high gas fractions $\mu(t)$. Assuming a constant star formation efficiency, this results in

an exponential decrease of subcloud mass with disk age t (e.g. Clayton 1985):

$$M_{\text{scl}} = M_{\text{scl}}(0) \exp(-t/t_{\text{dec}}) \quad (1)$$

where $M_{\text{scl}}(0)$ is the mass of a subcloud formed at $t=0$ (which may vary between different models) and t_{dec} a characteristic time scale at which the mass of subsequent subclouds formed is assumed to decay (identical for all models). The assumption of a star formation rate (SFR) directly proportional to the subcloud formation rate is not essential for the results discussed here.

The decay time scale t_{dec} is constrained observationally by the ratio of the average past to present SFR in the Galactic disk ($\sim 3-7$; e.g. Mayor & Martinet 1977; Dopita 1990). We here assume an exponentially decaying SFR with $t_{\text{dec}} = 6$ Gyr. As will be shown in Sect. 4.1, this SFR can account simultaneously for the actual gas-to-total mass-ratio in the disk of $\mu_1 \sim 0.05-0.2$ (Kulkarni & Heiles 1987; Binney & Tremaine 1987; see also Basu & Rana 1992), the smooth increase in the global AMR for elements such as O and Fe, and the magnitude of the current SFR in the Galactic disk (i.e. $\sim 3.5 M_{\odot} \text{ yr}^{-1}$; e.g. Dopita 1987). In contrast, constant SFR models are inconsistent with these observations (Twarog 1980a; see also Clayton 1985).

The time between the formation and complete mixing of a subcloud to the inactive cloud part is defined as Δt_{mix} . This time scale has been considered to allow for the individual chemical evolution of a subcloud isolated from the inactive ISM (see below).

- *Individual star formation events:* We assume the onset of star formation within each subcloud to coincide with the formation of the subcloud itself in case of the reference model. This results in a grid of regularly spaced star formation times $t_{\text{sf}} = t_{\text{scl}}$.

We define the core dispersal time Δt_{disp} as the time between onset of star formation t_{sf} within a subcloud core and the moment star formation ends due to the actual break up of this core. Observational estimates of this time scale are generally $\lesssim 10^7$ yr (e.g. Garmany et al. 1982; Leisawitz 1985; Genzel & Stutzki 1989; Rizzo & Bajaja 1994; Haikala 1995). For the reference model, we assume the *entire* subcloud to break up at time of dispersal of the star forming subcloud *core*, i.e. $\Delta t_{\text{mix}} = \Delta t_{\text{disp}}$.

The star formation efficiency ϵ^j is defined as the amount of subcloud matter ΔM_{scl} turned into stars during star formation event j . In fact, the star formation efficiency determines the amount of material to which the stellar ejecta of a previous stellar generation are mixed within a given star forming cloud. Observational estimates for ϵ in molecular clouds in the Galactic disk span a wide range: between a few tenths of a percent to $\sim 50\%$ (e.g. Wilking & Lada 1983). We will discuss the values assumed for ϵ^j in Sect. 4.

Sequential stellar enrichment is taken into account by assuming that a fraction λ^j of enriched material associated

with star formation event j is mixed homogeneously to the subcloud hosting the next star formation event. Subcloud material not converted into stars is mixed to the inactive cloud part after complete dispersal of the subcloud. The relative importance of these model parameters on the resulting stellar abundance variations will be discussed in Sect 4.2.

3.4. Stellar evolution data

We follow the stellar enrichment of the star forming cloud in terms of the characteristic element contributions of Asymptotic Giant Branch (AGB) stars, SNII, SNIa, and SNIb/c. This treatment is based on the specific abundance patterns observed within the ejecta of each of these stellar groups (e.g. Trimble 1991; Groenewegen & de Jong 1992; van den Hoek et al. 1996). We take into account metallicity dependent stellar element yields, remnant masses, and ages, while assuming the stellar ejecta to be returned at the end of the lifetime of the star (see e.g. Maeder 1992; Schaller et al. 1992). The respective time delays in enrichment by SNIa and SNII are accounted for in detail. A more detailed description of the combined set is given elsewhere (e.g. van den Hoek et al. 1996; see also electronic version of this paper).

For AGB stars (initial mass $m \lesssim 8 M_{\odot}$) we adopt the metallicity dependent yields presented by Groenewegen & de Jong (1992). These yields are based on a synthetic evolution model for AGB stars and are successful in explaining the observed abundances in carbon stars and planetary nebulae in the Galactic disk (Groenewegen et al. 1995). For Type-II SNe, we use the explosive nucleosynthesis yields (independent of initial metallicity) described in detail by Hashimoto et al. (1993) and Thielemann et al. (1993) for stars with $8 \lesssim m[M_{\odot}] \lesssim 60$. The $20 M_{\odot}$ model of this set accounts well for the observed abundances in SN1987A (Nomoto et al. 1991). Explosive nucleosynthesis yields for Type-Ia SNe are adopted from Nomoto et al. (1984; model W7 for SNIa at $Z = Z_{\odot}$ and $Z = 0.0$ of the accreted material; see also Yamaoka 1993) and for SNIb/c from Woosley et al. (1995). According to these yields, typical amounts of iron produced are $\sim 0.08 M_{\odot}$ for SNII, $\sim 0.8 M_{\odot}$ for SNIa, and $\sim 0.1 M_{\odot}$ for SNIb/c.

The adopted yields for SNIa, b/c are relatively uncertain due to unknown details of the progenitor history and the explosion mechanism (either binary or single star evolution; see e.g. Smecker-Hane & Wyse 1992; Woosley et al. 1993). However, we do not believe that these uncertainties are relevant for the qualitative results obtained in this paper (cf. Sect. 5.2).

Metallicity dependent stellar yields for stars during their wind (i.e. pre-SN) phase have been adopted from Maeder (1992, 1993), to whom we refer the reader also for a definition of the stellar element yields as used in the Appendix. For stars with $m \gtrsim 20 M_{\odot}$ we used the higher mass loss rates in case $Z=0.02$ (cf. Maeder 1992; Schaller

et al. 1992). The mass m_{α} of the helium core left at the end of the He-burning phase (or C-burning phase for massive stars) has been used as input for the SNII and SNIb/c nucleosynthesis models referred to above. Yields were linearly interpolated both in m and m_{α} . Errors due to the coupling of these sets of stellar evolution data are probably small and are neglected here (cf. van den Hoek et al. 1996). Remnant masses and stellar lifetimes were adopted from the Geneva group as well (e.g. Schaller et al. 1992).

For the reference model, the adopted IMF-slope, stellar mass limits at birth, and progenitor mass ranges for stars ending their lives as SNIa and SNII(+SNIb/c) are listed in Table 2. Stars with $m > 60 M_{\odot}$ have been excluded because their theoretical yields are rather uncertain (e.g. Maeder 1992). We expect that the IMF-weighted contribution by such stars to the enrichment of the ISM is relatively low. Stars more massive than $m_{\text{u}}^{\text{SNII}}$ are assumed not to explode as supernova but to end as black hole (cf. Maeder 1992; Nomoto et al. 1994; Prantzos 1994; Tsujimoto et al. 1995). Consequently, stars with $m \gtrsim m_{\text{u}}^{\text{SNII}}$ contribute to the ISM enrichment during their stellar wind phase only. When no upper mass limit $m_{\text{u}}^{\text{SNII}} = 25\text{--}30 M_{\odot}$ is introduced, models using up-to-date SNII yields predict abundances that are too high compared to those observed in the ISM, in particular for helium and oxygen (e.g. Twarog & Wheeler 1982; Maeder 1992, 1993; Timmes et al. 1995).

We consider a fraction $\phi^{\text{SNIa}} = 0.005$ of all WD progenitors with initial mass between ~ 2.5 and $8 M_{\odot}$ to end as SNIa. A more detailed discussion of the contribution by SNIa is postponed to Sect. 5.1 (see also Ishimaru & Arimoto 1995). In addition, we assume about one third of all supernova progenitors with $m_{\text{u}}^{\text{SNII}} \lesssim m \lesssim m_{\text{u}}^{\text{SNII}}$ to end as SNIb/c, i.e. $\phi^{\text{SNIb/c}} \equiv [\text{SNIb/c} / (\text{SNIb/c} + \text{SNII})] = 0.33$. This value is based on the observed ratio of current formation rates of SNII and SNIb/c in the Galaxy (e.g. van den Bergh & Tammann 1991; Tutukov, Yungelson & Iben 1992; Cappellaro et al. 1993).

4. Results

We present results for the inhomogeneous chemical evolution model described in the previous section. First, we consider the reference model which does not incorporate stellar abundance variations at a given age. Thereafter, we discuss models that do incorporate stellar abundance variations due to: 1) sequential stellar enrichment, 2) infall of metal-deficient matter, and 3) combined infall of metal-deficient matter and sequential enrichment.

4.1. Reference model

We consider a homogeneous gas cloud with initial conditions as listed in Tables 2 and 3. Within this cloud, active subclouds are formed at regular time intervals of $1.4 \cdot 10^8$ yr so that in total $N_{\text{cl}} = 100$ subclouds form during cloud

Table 1. List of input parameters (values listed for reference model)

<i>Cloud and inactive cloud part</i>		
M_{cl}	$5 \cdot 10^{10} M_{\odot}$	total cloud total mass
t_{ev}	14 Gyr	cloud evolution time
N_{sf}	100	total number of star formation events
N_{scl}	100	total number of subclouds formed
$X_{\text{qcl}}(0)$	H=0.76	initial cloud abundances; He=0.24
<i>For each subcloud i</i>		
t_{scl}	$1.4 \cdot 10^8$ yr	time at which subcloud is formed, i.e. each $t_{\text{ev}} / N_{\text{scl}} = 1.4 \cdot 10^8$ yr
M_{scl}	exp	exponentially decaying subcloud mass at time of formation ($M_{\text{scl}}(t=0) = 6 \cdot 10^9 M_{\odot}$)
$N_{\text{sf}}^{\text{max}}$	1	maximum number of SF events within one subcloud
Δt_{mix}	Δt_{disp}	mixing time of entire subcloud
<i>For each star formation event j</i>		
t_{sf}	t_{scl}	evolution time at which SF-event j occurs
Δt_{disp}	10^7 yr	subcloud core dispersal time
ϵ	0.50	subcloud star formation efficiency ⁽¹⁾
λ	0	efficiency of sequential enrichment ⁽²⁾

Notes: (1) ϵ^j is the mass fraction of the subcloud converted into stars during dispersal time Δt_{disp}^j , (2) λ^j refers to the amount of stellar material returned to the subcloud core hosting the *next* star formation event.

Table 2. IMF related parameters and stellar enrichment

γ	-2.35	slope of power-law IMF m^{γ}
m_l, m_u	0.1, 60 M_{\odot}	stellar mass limits at birth
$m_l^{\text{SNII}}, m_u^{\text{SNII}}$	8, 30 M_{\odot}	progenitor mass range for SNII and SNIb/c
$m_l^{\text{SNIa}}, m_u^{\text{SNIa}}$	2.5, 8 M_{\odot}	progenitor mass range for SNIa
ϕ^{SNIa}	0.005	fraction of progenitors ending as SNIa
$\phi^{\text{SNIb/c}}$	0.33	fraction of SNII progenitors ending as SNIb/c

evolution time $t_{\text{ev}} = 14$ Gyr. We assume no time-delay between the formation of the subcloud and the actual onset of star formation within that subcloud, i.e. $t_{\text{sf}} = t_{\text{scl}}$, and further assume each subcloud to experience a single star formation event. During this event, lasting $\Delta t_{\text{disp}} = 10^7$ yr, half of the subcloud mass is converted into stars, i.e. $\epsilon = 0.50$. After each event, both gas and stars contained within the subcloud are mixed homogeneously to the inactive cloud part. We note that the assumption of $\epsilon = 0.50$ has no physical meaning here other than defining the gas consumption rate as a function of cloud age. Model related quantities are given in Table 3 (see Sect. 5.2).

Figure 3a shows resulting stellar and gas-to-total mass-ratios vs. age for the reference model. According to the assumed variation of subcloud mass with cloud evolution time (cf. Sect. 3.2), the gas-to-total mass-ratio decreases exponentially from $\mu_{\text{cl}} = 1$ to 0.1 (corresponding decrease in subcloud mass converted into stars is shown in Fig. 3b). Figure 3b illustrates that the amount of gas returned by

massive stars during each star formation event is less than $\sim 5\%$ of the total amount of gas converted into stars during the same event. This ratio is determined primarily by t_{sf} and ϵ (see below). The amount of gas returned during Δt_{disp} by the *entire* stellar population within the inactive cloud part vs. cloud age is plotted for comparison.

Corresponding stellar and interstellar [Fe/H] and [O/H] abundance ratios are shown in Figs. 4a and b, respectively. At a given age, stellar and ISM abundances are exactly the same so that abundance inhomogeneities do not occur. Note that the resulting AMRs do not depend on the adopted value for M_{cl} as long as the normalisation of the SFR remains such that the condition of a current gas-to-total mass-ratio μ_1 of 0.1 is met. The reference model predicts [Fe/H] and [O/H] abundance ratios that are consistent with the mean EDV data for stars younger than ~ 10 Gyr. For stars older than 10 Gyr, agreement with the observations may be improved e.g. by considering cloud ages in excess of $t_{\text{ev}} = 14$ Gyr or by detailed modeling of the halo-disk enrichment at early epochs of Galaxy

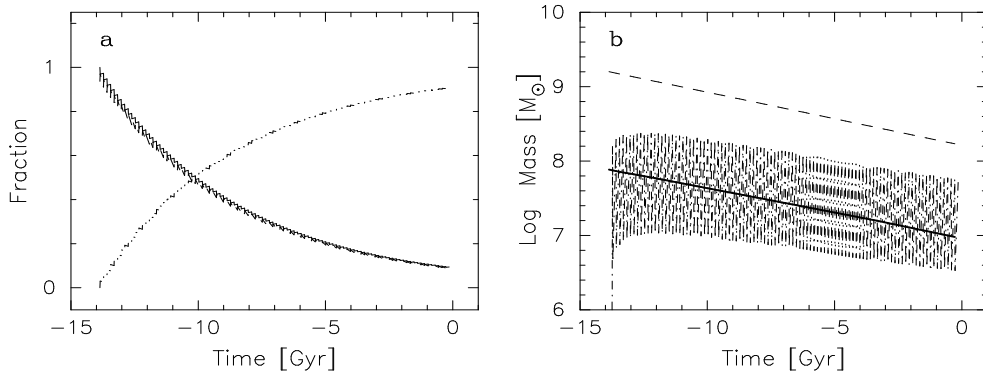


Fig. 3. Reference model: **a** Stellar-to-total (dashed curve) and gas-to-total (solid line) mass-ratios vs. age. The gas-to-total mass-ratio for the inactive cloud part coincides with that for the entire cloud, **b** Subcloud mass $\Delta M_{\text{scl}} = \epsilon M_{\text{scl}}$ converted into stars (dashed curve) and amount of gas returned to the subcloud by newly formed stars within Δt_{sf} (solid curve) vs. age. We assumed $M_{\text{scl}}(t = 0) = 6 \cdot 10^9 M_{\odot}$. Total mass returned by previously formed stellar populations present in the inactive cloud is shown for comparison (dash-dotted curve). Fluctuations in this curve result from integration over different time intervals, i.e. Δt_{sf} and t_{scl} (cf. Table 1).

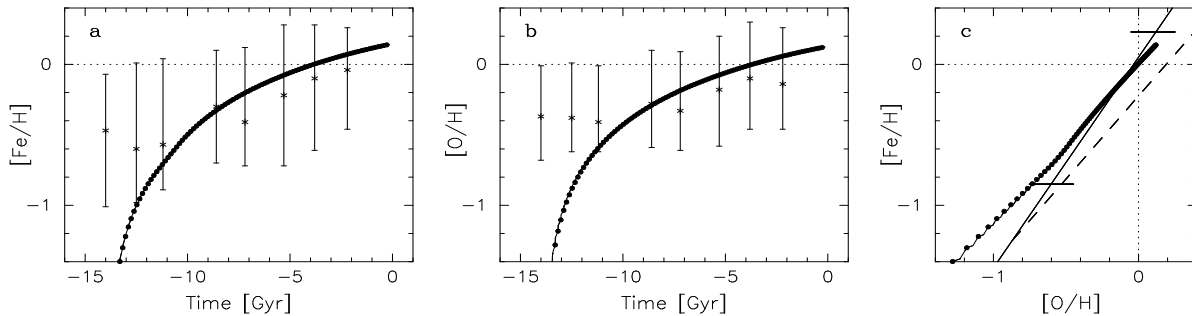


Fig. 4. Reference model: Stellar [Fe/H] and [O/H] abundance ratios vs. age. Stellar and ISM abundances at a given age are exactly the same. **a** [Fe/H]: stellar abundances at birth (full circles) coinciding with ISM abundances (solid curve). Each full circle represents a stellar generation with total mass of approximately ΔM_{scl} . Asterisks with error bars indicate the maximum stellar abundance variations observed in the Edvardsson et al. (1993a) data for main-sequence F and G dwarfs (averaged over 1.5 Gyr bins). Data for stars older than 15 Gyr have been omitted because of incompleteness (see Sect. 2). **b** [O/H]: curves and data similar to those for [Fe/H]. **c** Theoretical [Fe/H] vs. [O/H]-relations including SNIa (full circles) and excluding SNIa (dashed curve). Mean [Fe/H] vs. [O/H] relation for the Edvardsson et al. data is shown as a straight line (horizontal marks indicate the observational range)

evolution. We here concentrate on the stellar abundances observed during the last 10 Gyr of Galactic disk evolution.

Our adopted values of $\phi^{\text{SNIa}} = 0.005$ and $m_{\text{u}}^{\text{SNII}} = 30 M_{\odot}$ provide optimal consistency with the mean observed [Fe/H] vs. [O/H] relation (cf. Fig. 4c). Clearly, the slope of the resulting [Fe/H] vs. [O/H] relation in case of enrichment by SNII only ($m_{\text{u}}^{\text{SNII}} = 60 M_{\odot}$) is inconsistent with the observations. Thus, the data provided by Edvardsson et al. imply that SNII and SNIa,b/c nucleo-synthesis sites mixed their products together well. In addition, dilution of the supernova ejecta by more metal-deficient material is needed to comply with the range in [Fe/H] and [O/H] observed for F and G dwarfs in the SNBH. This is simply

because theoretically predicted (lifetime-integrated) mean [Fe/H] ratios within the ejecta of supernova progenitors are in general much larger than those observed for long-living stars in the SNBH (see Sect. 3.4). Thus, whatever process is responsible for the observed stellar abundance variations, both mixing of ejecta from different SN-types and dilution with metal-deficient material are involved.

The resulting well-defined tight AMRs for the reference model are similar to those predicted by conventional single-zone chemical evolution models (e.g. Twarog 1980a; Tinsley 1980). Such models account for the global chemical enrichment of the Galactic disk ISM during the last 10 Gyr, at least for elements like O and Fe, but they ob-

Table 3. Summary of model input parameters and resulting quantities related to the SFR (*scaled to $M_{\text{cl}} = 2 \cdot 10^{11} M_{\odot}$)

Model	Fig.	$M_{\text{scl}}(0)$ [M_{\odot}]	N_{sf}	ϵ^{max}	$m_{\text{u}}^{\text{SNII}}$ [M_{\odot}]	μ_1	SFR ₁ [$M_{\odot} \text{ yr}^{-1}$]	INF ₁ [$M_{\odot} \text{ yr}^{-1}$]	R^{SNII} [yr^{-1}]	R^{SNIa} [yr^{-1}]
Reference	3+4	1.3 (10)	100	0.50	30	0.09	2.9	–	1.3 (-2)	7.1 (-4)
Sequential (single)	5-1, 5-2	2.1 (10)	100	0.95	25	0.11	3.7	–	1.5 (-2)	8.2 (-4)
Sequential (multiple)	5-3	1.5 (10)	200	0.50	25	0.21	2.5	–	1.0 (-2)	6.4 (-4)
Infall	6	6.3 (9)	100	0.95	40	0.16	5.4	3.1	2.5 (-2)	1.6 (-3)
Infall+Sequential	7-1, 7-2	6.4 (9)	136	0.90	25	0.19	5.2	1.8	2.1 (-2)	1.3 (-3)
Infall+Sequential	7-3	6.4 (9)	166	0.90	25	0.32	4.4	3.1	1.8 (-2)	1.1 (-3)
Observations*						0.05–0.2	3.6±1.	≥0.5	2–4 (-2)	≥3 (-3)

***References:**

M_{cl} : Bahcall & Soneira (1980); Fich & Tremaine (1991).

μ_1 : Kulkarni & Heiles (1987); Binney & Tremaine (1987); see also Basu & Rana (1992).

SFR: Dopita (1987); Walterbos (1988; based on IR observations); Mezger 1988

INF: Mirabel & Morras (1984); Lépine & Duvert (1994).

SNII & SNIa: van den Bergh & Tammann (1991); Tutukov et al. (1992); Cappellaro et al. (1993); Strom (1993).

viously provide no explanation for the observed variations in stellar abundances at a given age.

4.2. Sequential stellar enrichment

In case of sequential star formation, efficient self-enrichment of a star forming gas cloud by successive stellar generations may result in abundance enhancements relative to the abundances in the ambient ISM. When the local mixing time scale is larger than the time between two successive star formation events in such a cloud, these abundance enhancements can be deposited and recorded by newly formed stars.

In our model, the impact of sequential enrichment on abundance inhomogeneities in the ISM is determined by: a) the dispersal time of the star forming region, b) the total number of stellar generations formed within one and the same cloud, c) the efficiency of sequential enrichment, i.e. the mass-ratio of the enriched stellar material and the cloud to which this material is mixed, d) details of stellar enrichment: e.g. the relative number of SNII and SNIa, and e) the IMF and stellar mass limits at birth. We distinguish the effect of single and multiple sequential stellar enrichment on the stellar abundance variations. We will refer to single sequential enrichment as the case in which a star formation event induces subsequent star formation in a nearby cloud (when mixing enriched material to this cloud).

4.2.1. Single sequential stellar enrichment

We present results for models incorporating single sequential stellar enrichment ($N_{\text{sf}}^{\text{max}} = 1$). For illustration purposes, we consider only the alternating half of the subclouds to experience sequential enrichment. We define ini-

tial masses of subclouds that are sequentially enriched as $M_{\text{scl}} \equiv \vartheta M_*$ where M_* is the total mass of gas converted into stars during the previous enriching star formation event. Initial masses of subclouds not involved with sequential enrichment are assumed to decrease exponentially (as for the reference model).

To maximize the effect of sequential enrichment on the stellar abundance variations, we assume $\vartheta = 0.2$, $\epsilon = 0.95$, $m_{\text{u}}^{\text{SNII}} = 25 M_{\odot}$, $\phi^{\text{SNIa}} = 0.005$, and an enrichment efficiency $\lambda = 0.95$ (i.e. nearly all enriched stellar material ejected is mixed to the material wherein the *next* star formation event is induced). We consider cloud dispersal times $\Delta t_{\text{disp}} \sim 10^7$ yr. Such dispersal times are among the largest ones deduced from observations of nearby star forming molecular clouds (see Sect. 3.3). Using a theoretical age vs. turnoff-mass relation (e.g. Schaller et al. 1992), Δt_{disp} can be related to the least massive star m_{enr} able to enrich material before cloud dispersal. For instance, values of $\Delta t_{\text{disp}} \sim 5 \cdot 10^6$, 10^7 , and $2 \cdot 10^7$ yr, correspond to $m_{\text{enr}} \sim 40$, 15, and $12 M_{\odot}$, respectively.

Figures 5-1 and 5-2 (top and center panels in Fig. 5, respectively) illustrate the effect of sequential enrichment on the stellar abundance variations for cloud dispersal times of $\Delta t_{\text{disp}} = 10^7$ and $2 \cdot 10^7$ yr, respectively. The extent to which sequential enrichment contributes to the stellar abundance variations is determined by the chemical evolution of the ambient ISM. In general, large cloud dispersal times give rise to efficient locking up of metals in long living stars and enhanced stellar abundance variations relative to the abundances in the ISM. Stellar abundance variations due to single sequential stellar enrichment are found to be maximal for $\Delta t_{\text{disp}} \sim 2 \cdot 10^7$ yr. Larger values of Δt_{disp} allow stars less massive than $m \sim 12 M_{\odot}$ to dilute the metal-rich ejecta of more massive stars (e.g. Hashimoto et al. 1993).

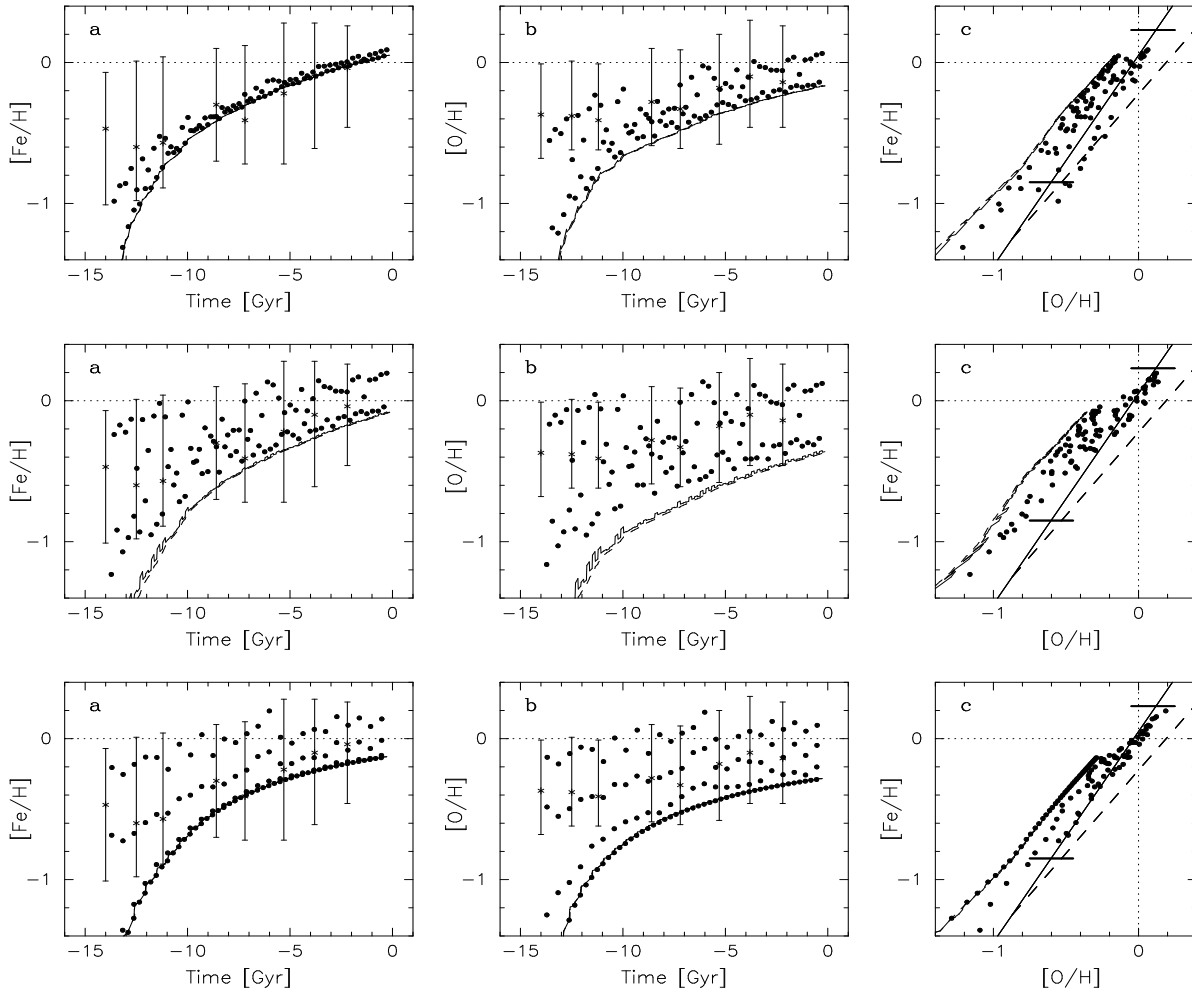


Fig. 5. Model results for single and multiple sequential stellar enrichment. *Top panels:* Single sequential enrichment assuming a cloud dispersal time $t_{\text{disp}} = 10^7$ yr. *Center panels:* Single sequential enrichment assuming $t_{\text{disp}} = 2 \cdot 10^7$ yr. *Bottom panels:* Multiple sequential enrichment (see text). Model results are shown for variations of stellar and interstellar $[\text{Fe}/\text{H}]$ and $[\text{O}/\text{H}]$ abundance ratios: **a** $[\text{Fe}/\text{H}]$ vs. age, **b** $[\text{O}/\text{H}]$ vs. age, **c** $[\text{Fe}/\text{H}]$ vs. $[\text{O}/\text{H}]$. Stellar abundances are indicated by filled circles. Mean interstellar abundances (averaged over both active *and* inactive clouds) are indicated by solid curves. Average interstellar abundances within the inactive cloud ISM only (indicated by short dashed curve) do approximately coincide with the overall mean abundances. Remaining symbols and curves have the same meaning as in Fig. 4

In case $\Delta t_{\text{disp}} = 2 \cdot 10^7$ yr, resulting stellar abundance variations due to sequential enrichment are sufficiently large to explain the observed variations in $[\text{O}/\text{H}]$. In contrast, corresponding variations in $[\text{Fe}/\text{H}]$ are much smaller than observed. This is true even though the models presented here do account for sequential enrichment by SNIb/c which usually show theoretical $[\text{O}/\text{Fe}]$ ratios much lower than SNI (e.g. Woosley et al. 1995). Results disagree with the observational fact that stellar abundance variations in $[\text{Fe}/\text{H}]$ are considerably larger than in $[\text{O}/\text{H}]$ (see also Gilmore & Wyse 1991; Edvardsson et al. 1993a). An enhanced contribution of SNIb/c (i.e. assuming $\phi_{\text{SNIb/c}} > 0.33$) or participation of SNIa to the process of sequential enrichment seems to be excluded by the ob-

servations (van den Bergh & Tammann 1991; Tutukov et al. 1992).

We conclude that single sequential stellar enrichment models are inconsistent with the observations because they: 1) result in $[\text{O}/\text{H}]$ variations that are larger than those in $[\text{Fe}/\text{H}]$, 2) predict current ISM abundances far below those observed, and 3) are difficult to reconcile with the apparent age independency of the stellar abundance variations (see Sect. 2). This conclusion is independent of the assumed cloud dispersion time scale Δt_{disp} , sequential enrichment efficiency λ , value of ϑ , background level of iron-group elements set by SNIa (i.e. ϕ^{SNIa}), star formation efficiency ϵ , and adopted IMF. Also, omitting the enrichment during the stellar wind phase of supernova progenitors does not alter this conclusion.

4.2.2. Multiple sequential stellar enrichment

The effect of sequential stellar enrichment on the abundance variations among successive stellar generations can be very large, especially for high sequential enrichment efficiencies and/or small amounts of cloud material to which the stellar ejecta are mixed before star formation is initiated. These conditions are naturally fulfilled when isolated gas clouds experience multiple star formation events (i.e. $N_{\text{sf}}^{\text{max}} > 1$) before mixing with the surrounding ISM. Since the gas content of an isolated cloud is reduced by each star formation event, cloud abundances rapidly increase when enriched by successive generations of massive stars.

We consider two possible scenarios of multiple sequential enrichment. In the first scenario, earlier generations of stars actually separate from the remaining subcloud material after dispersal of the subcloud core and do not further participate in the enrichment of the subcloud. Such models result in substantial stellar abundance variations only under conditions and assumptions similar to those for the single sequential enrichment case. In the second scenario, all stellar generations formed in the subcloud continue to contribute to the enrichment until the entire subcloud has been dispersed. In this case, large stellar abundance variations arise due to efficient recycling of the stellar ejecta from successive generations formed within the same cloud.

We apply the second scenario and consider all subclouds to experience multiple sequential enrichment. As maximum number of star formation events within one and the same subcloud we assume $N_{\text{sf}}^{\text{max}} = 4$ (e.g. suggested by observations of OB subgroups in Orion; see Blaauw 1991). We adopt a sequential enrichment efficiency $\lambda = 1$ (by definition within the same subcloud), a star formation efficiency ϵ between 0.3 and 0.6 for each star formation event, and $\Delta t_{\text{disp}} = 10^7$ yr. Other values of these parameters may provide similar results. Remaining model parameters are taken as for the single sequential enrichment model.

In Fig. 5-3, we plot resulting stellar abundance variations in case of multiple sequential stellar enrichment. Although variations caused by the first sequential enrichment event are relatively small (similar to the single sequential enrichment case assuming $\Delta t_{\text{disp}} = 10^7$ yr; see Fig. 5-1), abundance variations caused by subsequent events can be as large as ~ 0.2 – 0.3 dex (depending on the subcloud abundances). As mentioned before, such large abundance variations are mainly due to ongoing sequential enrichment of the remaining cloud material by stellar generations formed earlier in the cloud. We find that models incorporating multiple sequential stellar enrichment encounter the same problems as single sequential enrichment models. However, the former models appear observationally far more justified. This is true in particular for the sequential enrichment and star formation efficiencies, as well as the cloud core dispersal times, required to obtain a given stellar abundance variation.

We conclude that the observed stellar abundance variations are difficult to explain by sequential stellar enrichment only. This conclusion is not altered when allowing for variations in sequential enrichment between distinct star formation events (e.g. by considering variations in the IMF, relative formation rates of SNII and SNIb/c, etc.). Possible exceptions may be selective mixing of SNII nucleosynthesis products to the material wherein star formation is induced, and/or cloud conditions that determine both the composition of the ejecta returned by a stellar generation (e.g. by means of the IMF, $m_{\text{u}}^{\text{SNII}}$, Δt_{disp} , contribution by SNIb/c, binaries) and the sequential enrichment efficiency (and/or star formation efficiency). However, the impact of such conditions on the stellar abundance variations, which would imply that the IMF weighted SN yields used here would be considerably modified, is beyond the scope of this paper.

4.3. Episodic infall of metal-deficient matter

Infall of metal-poor material can account for abundances of newly formed stars which lie substantially below the abundances in the global disk ISM. In principle, abundance variations due to metal-deficient gas infall are determined by the abundances within the infalling gas, the gas infall rate, and the amount of disk ISM to which the infalling material is mixed before star formation is initiated. Stellar abundance variations due to infall of metal-rich material associated with SN ejecta from massive stars in the Galactic disk can be considered as a special case of sequential stellar enrichment and is not discussed here.

Element abundances within the infalling gas are constrained by the lowest abundances observed for disk stars with $[\text{Fe}/\text{H}] \gtrsim -1$. The Edvardsson et al. data imply infall abundances of $[\text{M}/\text{H}]_{\text{inf}} \lesssim -0.8$ to -1.2 for e.g. M=C, Mg, Al, and Si. These abundances are consistent with observations of interstellar clouds in the halo (see Sect. 5.2) and suggest that infall induced star formation is associated with the lowest abundances observed among disk F and G dwarfs in the SNBH. We assume infall abundances similar to the abundances observed among the oldest metal-poor disk stars, i.e. $[\text{Fe}/\text{H}] = -1$, $[\text{O}/\text{H}] = -0.65$, and a hydrogen mass fraction of $X \sim 0.72$ (e.g. Bessell et al. 1991). For simplicity, we do not account for abundance inhomogeneities within the infalling gas and assume infall abundances to be constant in time. Furthermore, we consider infall to occur as soon as the infall abundances are reached in the global disk ISM (presumably corresponding with the onset of star formation in the disk).

The detailed manner in which gas infall varies with time is not essential for the results presented here *as long as* infalling gas plays an important role in determining the stellar abundances when it induces star formation. Here, we deal with the concept of infall induced star formation, i.e. the infalling gas initiates star formation when falling onto the disk. This concept is based on observations of

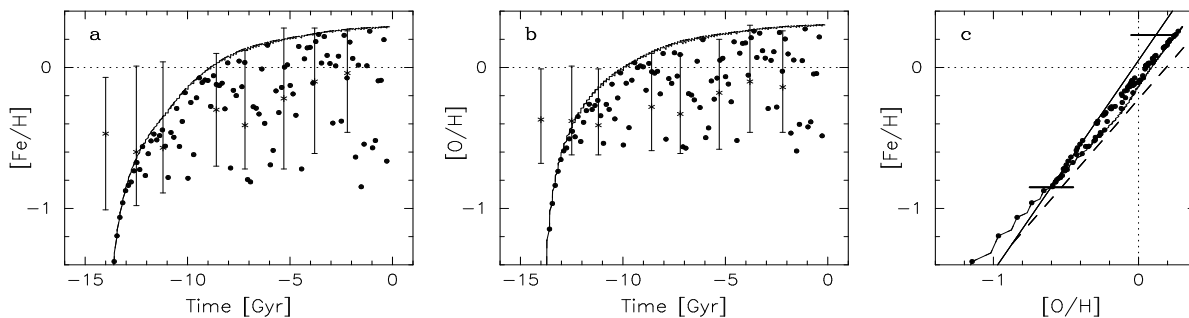


Fig. 6. Infall of metal-deficient material: model results are shown for variations of stellar and interstellar $[\text{Fe}/\text{H}]$ and $[\text{O}/\text{H}]$ abundance ratios: **a** $[\text{Fe}/\text{H}]$ vs. age, **b** $[\text{O}/\text{H}]$ vs. age, **c** $[\text{Fe}/\text{H}]$ vs. $[\text{O}/\text{H}]$. Symbols and curves have the same meaning as in Fig. 5

infalling high-velocity clouds that strongly interact with disk ISM and initiate star formation therein as soon the critical density for star formation is reached (see Sect. 5.2). Since star formation occurs by definition within active subclouds according to our model, infall is associated with subclouds experiencing star formation shortly after their formation. For simplicity, we assume each subcloud to contain an amount of infalling gas accumulated at the time star formation is induced. This amount is taken as a random fraction of the initial subcloud mass (i.e. between 0 and 1). In this manner, we allow for local and episodic gas infall onto the Galactic disk ISM. On average, the gas infall rate is assumed to decay exponentially on a time scale $t_{\text{dec}} = 6$ Gyr while its overall amplitude is constrained by $\mu_1 = 0.05\text{--}0.2$ (cf. Eq. (1); see Table 3).

We assume an initial disk mass $M_{\text{cl}} = 3 \cdot 10^{10} M_{\odot}$ before the onset of gas infall. This results in a disk initial-to-final mass-ratio $\zeta = 0.55$ according to an exponential decrease of subcloud mass with cloud evolution time ($M_{\text{scl}}(0) = 2 \cdot 10^9 M_{\odot}$; cf. Table 3). Clearly, stellar abundance variations due to metal-deficient gas infall are small at low levels of enrichment of the global disk ISM (i.e. large initial disk mass). Furthermore, continuous and large scale metal-deficient gas infall not associated with star formation results in relatively small stellar abundance variations. Thus, the magnitude of the stellar abundance variations is affected by the ratio of initial disk mass and total amount of infalling matter, as well as the amount of infalling gas that is involved with induced star formation in the disk ISM.

Figure 6 displays resulting AMRs for iron and oxygen in case of episodic infall of metal-deficient gas. We assumed $\phi^{\text{SNIa}} = 0.015$, $\phi^{\text{SNIb/c}} = 0.33$, and $m_{\text{u}}^{\text{SNI}} = 40 M_{\odot}$. The value of $m_{\text{u}}^{\text{SNI}}$ is taken larger than for the reference model (cf. Table 2) to obtain somewhat better agreement with the observations. Resulting abundances in the disk ISM follow the upper end of the abundances observed in F and G dwarfs younger than ~ 10 Gyr. Although the effect of global infall of metal deficient gas is generally to dilute the enrichment of the ISM, the inflow model results in

larger ISM abundances than the reference model. This is mainly due to: 1) the assumption of a low initial disk mass which allows for a rapid early enrichment of the disk, and 2) the assumption of *local* infall of metal-deficient gas and subsequent star formation therein so that infalling material has relatively small effect on the dilution of the *global* disk ISM.

By varying the ratio of infalling matter and disk ISM within each subcloud, stellar abundance variations of $\Delta [\text{Fe}/\text{H}] \sim 0.8$ dex and $\Delta [\text{O}/\text{H}] \sim 0.65$ dex naturally can be accounted for. In addition, the scatter in $[\text{Fe}/\text{H}]$ remains larger than in $[\text{O}/\text{H}]$ since the iron abundances within the infalling gas relative to solar (i.e. $[\text{Fe}/\text{H}]_{\text{inf}} = -1$) are much smaller than that of oxygen ($[\text{O}/\text{H}]_{\text{inf}} = -0.65$). We note that the current gas infall rate of $\sim 3.1 M_{\odot} \text{ yr}^{-1}$ predicted by the model shown in Fig. 6 is larger than suggested by the observations (see Sect. 5.1). However, other choices of model parameters, e.g. ζ , predict much lower infall rates while providing similar abundance results.

Our models incorporating metal-deficient gas infall are in good agreement with the observed magnitude of stellar abundance variations and the slope of the $[\text{Fe}/\text{H}]$ vs. $[\text{O}/\text{H}]$ relation observed. However, these models predict current interstellar $[\text{Fe}/\text{H}]$ and $[\text{O}/\text{H}]$ abundance ratios of ~ 0.2 dex *above* solar. This is in marked contrast with $[\text{O}/\text{H}]$ abundance ratios of ~ 0.15 dex *below* solar observed both in interstellar gas and recently formed stars in the SNBH (see Sect. 2). In addition, these models appear to disagree with the observations on two other grounds. First, no significant scatter in the $[\text{Fe}/\text{H}]$ vs. $[\text{O}/\text{H}]$ relation is predicted, contrary to what is observed for intermediate age disk stars (cf. Fig. 1). Part of the observed scatter may be due to experimental errors but variations of at least ± 0.1 dex in the $[\text{Fe}/\text{H}]$ vs. $[\text{O}/\text{H}]$ relation are probably real and have to be explained by any satisfactory model. A way to account for such scatter would be to allow for considerable abundance variations among different parcels of infalling gas. Secondly, these models predict stellar abundance variations to increase with time. This is inconsistent with the apparent constancy of the abundance scatter ob-

served. Possible ways out may be uncertainties in the ages of stars older than ~ 10 Gyr or disk evolution times in excess of $t_{\text{ev}} \sim 14$ Gyr.

We conclude that models dealing with metal-deficient gas infall can probably be excluded as the complete answer to the stellar abundance variations observed, even though such models are in good agreement with both the observed abundance variations and $[\text{Fe}/\text{H}]$ vs. $[\text{O}/\text{H}]$ relation. This conclusion is primarily based on the fact that such models predict mean current ISM abundances ~ 0.4 dex larger than those observed in the SNBH.

4.4. Metal-poor gas infall combined with sequential enrichment

Motivated by the results previously discussed, we study the combined effect of sequential stellar enrichment and episodic infall of metal-deficient gas on the inhomogeneous chemical evolution of the Galactic disk. Such investigation is important also because these processes are observed to operate simultaneously in the SNBH (see Sect. 5.2).

Attractive features of combined infall of metal-poor gas and sequential stellar enrichment are that a self-consistent explanation can be obtained for: 1) the presence of high metallicity stars at early epochs of star formation in the Galactic disk (due to sequential enrichment), 2) the presence of metal-poor stars at recent epochs of Galactic evolution (as a result of metal-deficient gas infall), 3) the nearly constant magnitude of the stellar abundance variations during the lifetime of the disk, and 4) abundances in the local disk ISM that are currently below solar (as observed for oxygen).

We show in Fig. 7 results for combined sequential stellar enrichment and metal-deficient gas infall. Model assumptions concerning each of these processes are similar to those described in the previous sections (e.g. $\epsilon^{\text{max}} = 0.90$, $\lambda = 0.95$, $m_{\text{u}}^{\text{SNII}} = 25 M_{\odot}$, $\phi^{\text{SNIa}} = 0.005$, and $\phi^{\text{SNIb/c}} = 0.33$; cf. Tables 2 and 3). The three models shown in Fig. 7 differ only in the amounts of disk ISM involved with sequential stellar enrichment and infalling gas accreted during the lifetime of the disk. For each of these models, resulting stellar abundance variations and $[\text{Fe}/\text{H}]$ vs. $[\text{O}/\text{H}]$ relation are consistent with the observations. Clearly, models with combined sequential enrichment and metal-poor gas infall do not encounter the specific problems involved when each of these processes is considered separately.

We study the relative impact of metal-poor gas infall and sequential stellar enrichment on the resulting stellar abundance variations as well as the global enrichment of the ISM. First, we investigate the effect of varying the fraction of subclouds (i.e. the amount of star forming disk ISM) experiencing multiple sequential stellar enrichment ($N_{\text{sf}}^{\text{max}}=4$, $\Delta t_{\text{disp}} = 10^7$ yr, $\epsilon^{\text{max}} = 0.9$; see Sect. 4.2). This fraction increases from $\sim 10\%$ to $\sim 25\%$ when going from top to center models shown in Fig. 7. The remaining part

of the subclouds is assumed to experience one single star formation event. Furthermore, we assume half of the subclouds to form stars partly from infall of metal-deficient gas (i.e. Figs. 7-1 and 7-2), regardless of the number of star formation events in each subcloud. Note that subclouds involved with metal-poor gas infall form predominantly stars with abundances below those in the global disk ISM. It can be seen that mean interstellar abundances and stellar abundance variations are not significantly altered when the fraction of ISM associated with sequential stellar enrichment is increased from 10 to 25%. However, when this fraction is further increased, more and more metals will be locked up in long living stars due to sequential enrichment and marked deviations from the observed $[\text{Fe}/\text{H}]$ vs. $[\text{O}/\text{H}]$ relation will occur (see Sect. 4.2).

Secondly, we investigate the effect when the fraction of subclouds forming stars from metal-deficient gas infall is increased from 50 to 100%. In this case, stellar generations are all formed according to infall induced sequential star formation and the total mass of infalling gas is increased by a factor two. This results in a reduction of the interstellar $[\text{Fe}/\text{H}]$ and $[\text{O}/\text{H}]$ abundance ratios by ~ 0.1 dex (see Fig. 7-3). Interestingly, this marginally affects the magnitude of the resulting stellar abundance variations (assuming $\epsilon^{\text{max}} = 0.9$, $\lambda = 0.95$) but strongly alters the number of stars with abundances below those present in the global disk ISM. We note that direct comparison of the abundance results with previous models is not justified because the enhanced gas infall model results in a current gas-to-total mass-ratio $\mu_1 \sim 0.3$, i.e. considerably higher than the $\mu_1 = 0.1-0.2$ indicated by the observations (cf. Table 3). To arrive at $\mu_1 = 0.2$, a reduction in initial disk mass from $3 \cdot 10^{10}$ to $2 \cdot 10^{10} M_{\odot}$ would be required. In turn, this would result in ISM abundances and stellar abundance variations similar to that for models with more modest infall rates.

4.5. Additional abundance constraints

Keeping these results in mind, we study how models with combined sequential stellar enrichment and metal-poor gas infall behave when confronted with additional observational constraints provided by the stellar abundance variations and current ISM abundances of C, Mg, Al, and Si.

Carbon abundance data for 85 F and G dwarfs in the SNBH have been presented by Andersson & Edvardsson (1994). These data show that there is a weak correlation between $[\text{C}/\text{H}]$ and $[\text{O}/\text{H}]$ (see Fig. 8). The shape of this correlation differs from that between e.g. $[\text{Fe}/\text{H}]$ and $[\text{O}/\text{H}]$. In addition, the variation in $[\text{C}/\text{H}]$ (i.e. $\gtrsim 0.6$ dex) at a given value of $[\text{O}/\text{H}]$ is about three times larger than that in $[\text{Fe}/\text{H}]$.

If the observed stellar abundance variations are caused by infall of metal-deficient gas only, one would expect that stellar abundances for all elements heavier than helium would be mutually correlated, e.g. similar to the correla-

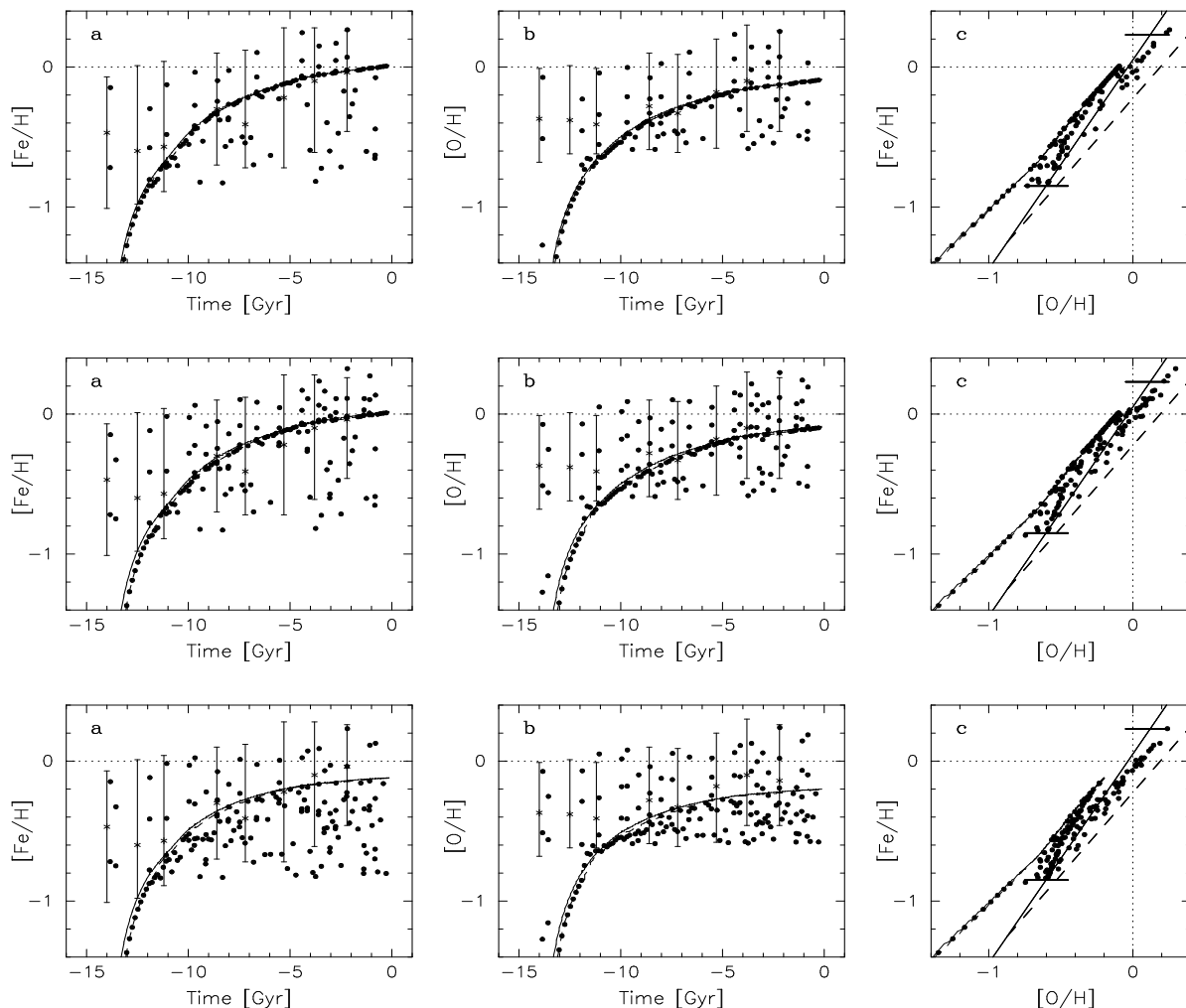


Fig. 7. Model results for combined sequential stellar enrichment and episodic infall of metal-poor gas. *Top panels:* $\sim 10\%$ of the clouds is assumed to experience multiple sequential enrichment while half of the subclouds is involved with metal-deficient gas infall. Nearly 5% of the clouds undergoes *both* infall of metal-deficient material and sequential stellar enrichment. *Center panels:* 25% of the subclouds experiences multiple sequential enrichment while half of the subclouds is involved with metal-poor gas infall. *Bottom panels:* as center panels but *all* subclouds experience metal-deficient gas infall. Model results are shown for variations of stellar and interstellar $[\text{Fe}/\text{H}]$ and $[\text{O}/\text{H}]$ abundance ratios: **a** $[\text{Fe}/\text{H}]$ vs. age, **b** $[\text{O}/\text{H}]$ vs. age, **c** $[\text{Fe}/\text{H}]$ vs. $[\text{O}/\text{H}]$. Symbols and curves have the same meaning as in Fig. 5

tion between oxygen and iron. In case of sequential stellar enrichment only, a similar behaviour would be expected only for elements that are produced predominantly by SNIi and SNIb/c. This implies that abundance-abundance variations between elements which are not synthesized predominantly within SNIi and SNIb/c (such as C and N), on the one hand, and elements that are produced predominantly within supernovae (e.g. O, Si), on the other hand, may be conclusive about the importance of metal-deficient gas infall.

We show in Fig. 8 results for: 1) infall of metal-deficient gas only (cf. Fig. 6), 2) multiple sequential stellar enrichment only (cf. Fig. 5-1), and 3) combined metal-poor gas infall and sequential enrichment (cf. Fig. 7-1). The in-

fall model predicts no substantial scatter in the $[\text{C}/\text{H}]$ vs. $[\text{O}/\text{H}]$ relation but follows the trend in the observations well. Although the scatter in the $[\text{C}/\text{H}]$ vs. $[\text{O}/\text{H}]$ relation suggests that infall is not exclusively responsible for the observed variations, the shape of this relation indicates that infall is important. Conversely, the sequential enrichment model shows large scatter in the $[\text{C}/\text{H}]$ vs. $[\text{O}/\text{H}]$ relation but appears to deviate from the observed trend. The correlation predicted by the combined sequential enrichment and infall model appears in reasonable agreement with the observations. However, the observed carbon abundances at $[\text{C}/\text{H}] \sim 0$ exhibit considerable more scatter than predicted by the model shown in Fig. 7-1 and seem to require a somewhat steeper increase of carbon relative to

oxygen. This may be due to variations in sequential stellar enrichment between different star formation events and/or variations in abundances within the infalling material.

In our models, the overall shape of the stellar $[C/H]$ vs. $[O/H]$ relation is due to infall of metal-poor material with carbon abundances $[C/O]_{\text{inf}} \approx -0.4$. The reason why these relatively low carbon infall abundances are necessary to explain the observed trend in the $[C/H]$ vs. $[O/H]$ relation, is unclear. A possible explanation may be a delayed carbon enrichment of the disk ISM, e.g. by low-mass SNIa progenitors that experience incomplete carbon burning or by low-mass AGB stars with small carbon yields.

Sequential stellar enrichment seems inevitable to explain the observed scatter in the $[C/H]$ vs. $[O/H]$ relation. Although large abundance inhomogeneities within the infalling gas may reproduce the observed variations as well, such inhomogeneities in $[C/O]$ appear inconsistent with the small scatter observed in e.g. $[Fe/O]$. Also, uncertainties in the derived carbon abundances may be considerably larger than those in O and Fe but are not likely to exceed ~ 0.2 dex (see Andersson & Edvardsson 1994; see also EDV). Therefore, it seems improbable that the scatter observed in the $[C/H]$ vs $[O/H]$ relation is due to observational errors. Finally, it is difficult to see how chemical differentiation processes (e.g. dust depletion, element mixing to the surface, O/N-cycle, metallicity dependent nucleosynthesis, etc.) can cause such large abundance-abundance variations among stars similar in mass and age.

From the arguments above, we conclude that models incorporating *both* infall of metal-poor gas and sequential stellar enrichment provide an adequate explanation for the observed $[C/H]$ vs. $[O/H]$ relation. For the model shown in Fig. 7-1, we compare the predicted stellar abundance ratios Si, Mg, and Al vs. Fe with the observations in Fig. 9. We find that slight offsets in $[M/H]$ are present between the model predicted and observed relations. These offsets, most pronounced for Al, are due to details in the adopted stellar yields and related parameters (see Table 3), and are not essential for the following discussion. Interestingly, a number of observed features are naturally reproduced by these models.

First, the observations suggest that variations in the stellar $[M/H]$ abundance ratios decrease with increasing metallicity. This is theoretically predicted by the individual effects of both sequential stellar enrichment and infall of metal-deficient material (as discussed above). For the model shown in Fig. 7-1, the resulting scatter in $[M/H]$ at a given value of e.g. $[Fe/H]$ is mainly due to sequential enrichment (except at abundances $[M/H] \lesssim -0.7$) and is strongly related to the iron contribution by SNIa in regions that do not experience sequential enrichment. It can be seen that the scatter in $[M/H]$ strongly decreases at solar metallicities and above. This may indicate that much of the observed element-to-element variations at high metallicities is due to observational errors of ~ 0.1 dex in $[M/H]$. Alternatively, the observed scatter at high metallicities

may imply that sequential enrichment by massive stars varies from one star formation event to another, e.g. by means of variations in the upper mass limit for SNII.

Secondly, the predicted variation in $[Mg/H]$ at a given $[Fe/H]$ is substantially larger than that in $[Si/H]$, consistent with the observations. In our model, this is due to: 1) the fact that part of the Si comes from SNIa which are important contributors also to Fe (Mg is produced less efficiently in SNIa than is Si by about one order of magnitude; e.g. Nomoto et al. 1984), and 2) the predicted ISM abundance of $[Mg/H]$ is less by about 0.1 dex than that of $[Si/H]$ (see Fig. 9).

Thirdly, the observed variation in $[Al/H]$ is similar (or even larger) than that in $[Mg/H]$ (see EDV). This behaviour is also found for the model shown in Fig. 7-1. The predicted ISM abundance of Al is probably too low by ~ 0.1 dex so that the resulting abundance scatter would be slightly reduced when correcting for this. The impact of sequential stellar enrichment is more pronounced for Al than for Mg and Si, due to the somewhat lower ISM abundance of Al (even after correction). Overall, we conclude that the magnitudes of the resulting stellar variations in Si, Mg, and Al vs. Fe appear in reasonable agreement with the observations.

Comparison of variations in Mg, Si, and Al vs. O with the observations reveals a somewhat different picture from that vs. Fe. The observed variation of $[Mg/H]$ with $[O/H]$ has been shown in Fig. 1; Al and Si display a similar behaviour. No trend is observed for variations in the scatter in the $\Delta[M/H]$ vs. $[O/H]$ relation, in contrast to that in the $\Delta[M/H]$ vs. $[Fe/H]$ relation. Furthermore, the observations indicate mean variations in $[M/Fe]$ of the same magnitude as those in $[M/O]$. In contrast, the model shown in Fig. 7-1 predicts variations in Mg, Al, and Si vs. Fe that are *considerably larger* than those vs. O. This is simply due to the fact that a substantial fraction of Fe originates from SNIa. Therefore, models predict hardly any scatter in e.g. $[Mg/O]$ since both elements are synthesized predominantly within SNII (and SNIb/c). This implies that either the scatter in the observed $[Mg/H]$ vs. $[O/H]$ relation is due to observational errors or that an additional process is needed in the models to explain this scatter.

In the former case, there would be no reason to believe the variations observed in the $[M/H]$ vs. $[Fe/H]$ relations either. However, we have argued above that at least part of this scatter is real. In the latter case, an additional mechanism causing the scatter in $[M/O]$ could be variations from one star formation site to another in the enrichment by SNII (and SNIb/c). Alternatively, such variations could include variations in e.g. the IMF, upper mass limit for SNII, and/or the mass distribution of binaries. We have verified that such variations generally result in abundance-abundance scatter sufficiently large to account for the observed variations of 0.1 dex in $[M/O]$ and sufficiently small to have a negligible effect on the scatter observed in $[M/Fe]$. Clearly, element-to-element variations in

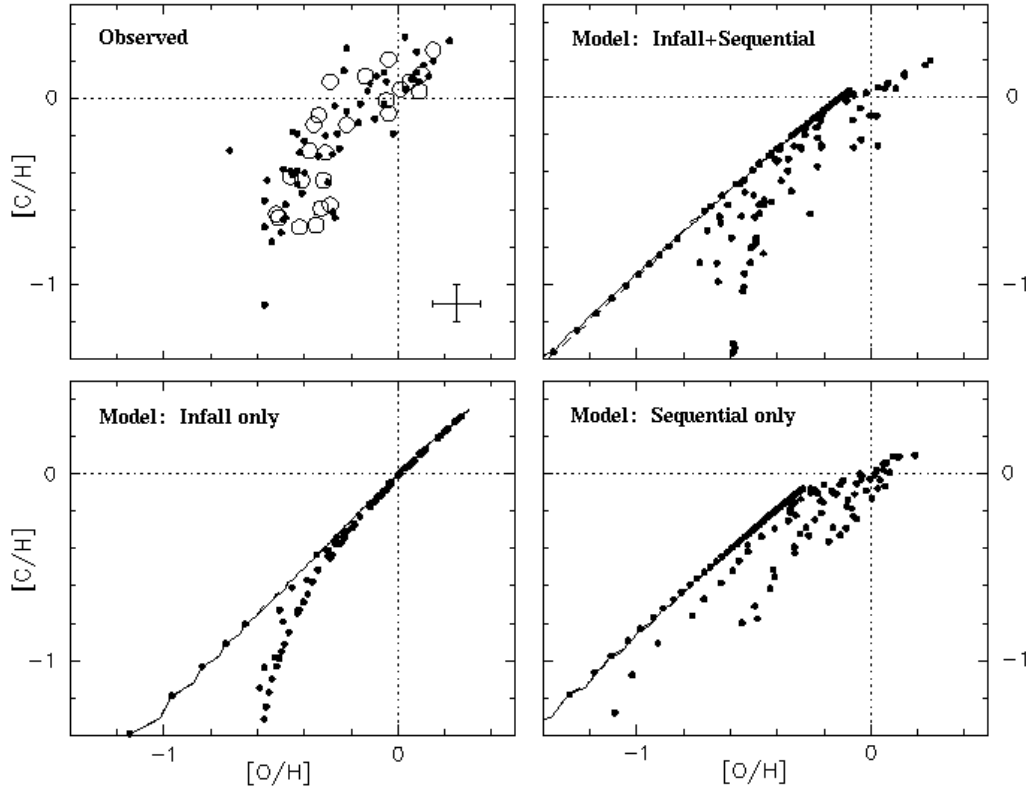


Fig. 8. Comparison between observed and model-predicted $[C/H]$ vs. $[O/H]$ relation. *Observations:* data for F and G dwarfs in the SNBH from Andersson & Edvardsson (1995). Open circles represent stars with mean stellar galactocentric distances at birth within 0.5 kpc from the Sun ($R_{\odot} = 8.4$ kpc). Full dots indicate stars with average distances within ~ 2 kpc from the Sun. Typical errors are indicated at the bottom right (top left panel). *Model results:* Predicted abundances of stars (full dots) and gas (solid line) for models incorporating metal-poor gas infall and/or sequential stellar enrichment

enrichment from one star formation site to another would be a natural refinement of the sequential stellar enrichment models discussed before.

We conclude that models incorporating both sequential stellar enrichment and episodic infall of metal-poor gas provide a natural explanation for the observed stellar abundance variations and are consistent with the ISM abundances of C, O, Fe, Mg, Si, and Al. We find that the mean ISM abundances and abundance-abundance relations can provide only limited constraints on the relative importance of sequential enrichment and infall induced star formation in the Galactic disk. Therefore, improvements in observational and theoretical constraints are required to disentangle the effects of these processes on the inhomogeneous chemical evolution of the Galactic disk in a more quantitative way.

5. Discussion

We briefly examine how the combined sequential stellar enrichment and metal-deficient gas infall models discussed in the previous section behave when confronted with inde-

pendent constraints provided by the current star formation rate in the Galactic disk and the chemical evolution of the Galactic halo. Thereafter, we discuss observational evidence in support of sequential enrichment and gas infall in the local disk ISM and consider possible implications of these processes for the chemical evolution of the Galaxy as a whole.

5.1. Additional constraints

5.1.1. SFR related constraints

The combined sequential enrichment and metal-deficient gas infall (Fig. 7-1) predicts a present SFR of $\sim 5.2 M_{\odot} \text{ yr}^{-1}$, and current rates of SNI (excluding SNIb/c) and SNIa of $R^{\text{SNI}} = 2.1 \cdot 10^{-2} \text{ yr}^{-1}$ and $R^{\text{SNIa}} = 1.3 \cdot 10^{-3} \text{ yr}^{-1}$, respectively. These values are roughly consistent with the observations (i.e. within a factor of two; see Table 3). Adopted values of $m_{\text{u}}^{\text{SNI}} = 25 M_{\odot}$ and $\psi^{\text{SNIa}} = 0.005$ may be somewhat too low since the SN-rates scale with the predicted SFR. For the same model, the current gas infall rate is determined by the assumed disk initial-to-final

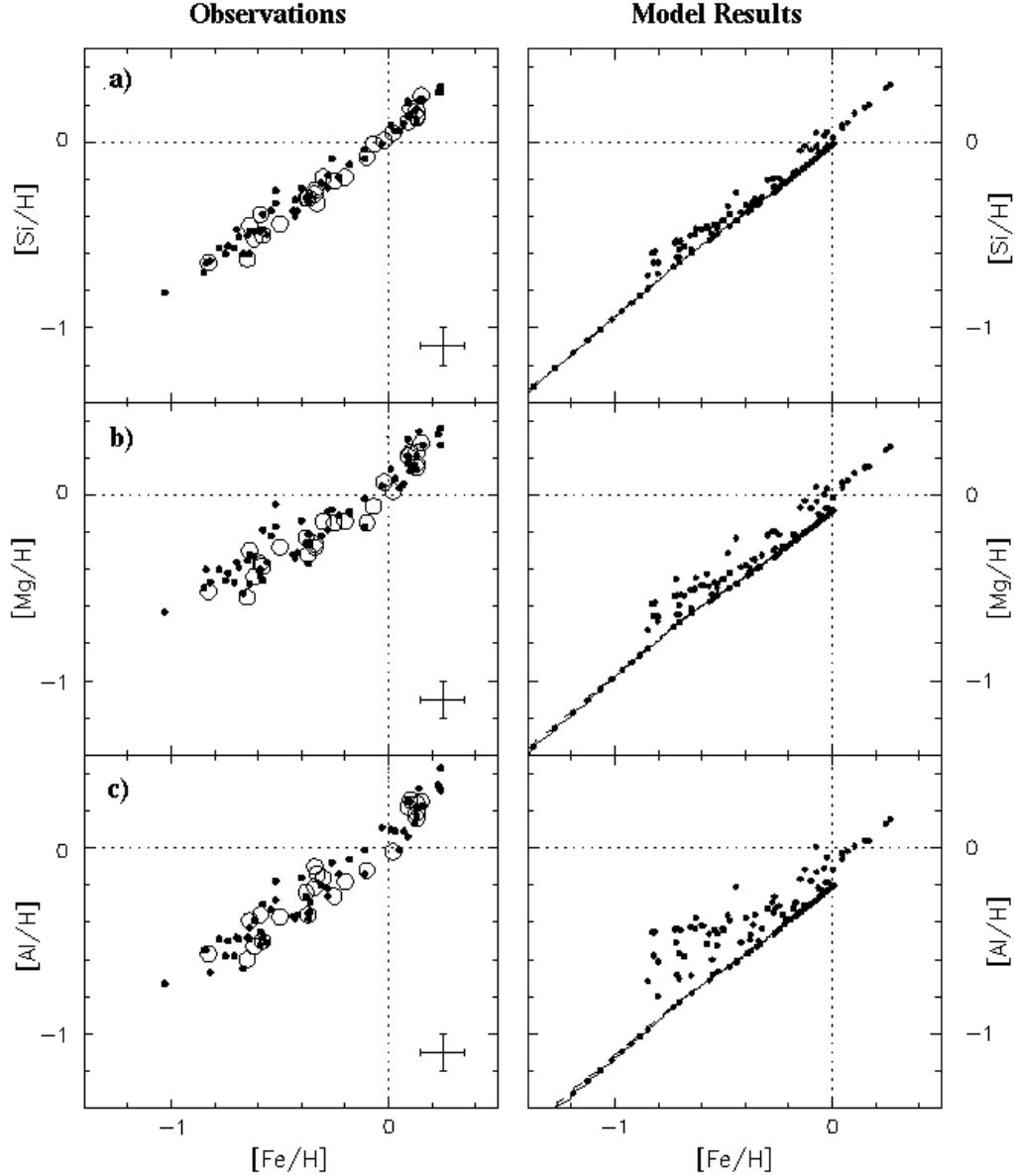


Fig. 9. Comparison between observed (left) and model-predicted (right) $[M/H]$ vs. $[Fe/H]$ relations: a) $[Si/Fe]$, b) $[Mg/Fe]$, and c) $[Al/Fe]$. *Observations*: data for F and G dwarfs in the SNBH from Edvardsson et al. (1993a). Symbols have the same meaning as in Fig. 8. Typical errors are indicated at the lower right of each panel. *Model results*: predicted abundances of stars (full dots) and gas (solid line) for model 7-1

mass-ratio $\zeta=0.5$ and by the time scale $\tau_{\text{inf}}=6$ Gyr on which infall decays exponentially. This results in a current gas infall rate of $1.8 M_{\odot} \text{ yr}^{-1}$. Observations indicate a current gas infall rate of $\sim 0.5 M_{\odot} \text{ yr}^{-1}$ (e.g. Mirabel & Morras 1984). However, selection effects may account for an underestimate of a factor of 2–3 (see Sect. 5.2). We note that higher values of ζ and/or lower values of τ_{inf} may apply equally well.

The predicted rates above all scale with the amplitude of the SFR. In turn, this amplitude is determined by the total cloud mass $M_{\text{cl}}=2 \cdot 10^{11} M_{\odot}$ and SFR decay time scale $t_{\text{decr}} \sim 6$ Gyr assumed (see Sect. 3.2). Distinct values of M_{cl} and/or t_{decr} will not affect the predicted stellar and interstellar abundances substantially, provided that a current gas-to-total mass-ratio $\mu_1 = 0.1$ is maintained. We conclude that the adopted parameters for the model shown in Fig. 7-1 are consistent with observational con-

straints on the current SFR, gas infall rate, and supernova rates. Obviously, these observations do not yet provide tight constraints on e.g. t_{decr} , μ_1 , and ζ , thus preventing a clear distinction between chemical evolution models based on these quantities (cf. Table 3).

5.1.2. Constraints related to the enrichment of the Galactic halo

The mean plateau value of $[\text{O}/\text{Fe}] \sim 0.5 \pm 0.15$ observed for halo stars with $[\text{Fe}/\text{H}] \lesssim -1$ (e.g. Bessell et al. 1991) is presumably determined by the average $[\text{O}/\text{Fe}]$ ratio within the ejecta of SNII (and SNIb/c) as well as the initial abundances within the halo ISM. For our models, the plateau value implies a maximum upper mass limit of SNII progenitors of $m_{\text{u}}^{\text{SNII}} \approx 40 M_{\odot}$, assuming initial metallicities $[\text{Fe}/\text{H}] \lesssim -1$, a Salpeter IMF, and stellar yields as described in Sect. 3.4. An even larger value for $m_{\text{u}}^{\text{SNII}}$ is implied when SNIb/c contributed substantially to the halo enrichment.

We assumed $m_{\text{u}}^{\text{SNII}} = 25 M_{\odot}$ for the combined infall + sequential enrichment model (Fig. 7-1) discussed before. This results in $[\text{O}/\text{Fe}] \sim 0.2$ at $[\text{Fe}/\text{H}] \lesssim -1$ while omitting the contribution from SNIb/c would have resulted in $[\text{O}/\text{Fe}] \sim 0.25$ at $[\text{Fe}/\text{H}] \lesssim -1$. This is inconsistent with the observations. Possible solutions to this discrepancy are: 1) $m_{\text{u}}^{\text{SNII}}$ and/or the IMF have changed between the time stars formed in the halo and the time of onset of star formation in the disk, 2) $m_{\text{u}}^{\text{SNII}}$ is actually $\sim 40 M_{\odot}$ for disk stars so that the predicted current disk ISM abundances of e.g. O and Fe increase and the effect of sequential enrichment is reduced, and/or 3) the adopted yields for SNII (and or SNIb/c) are in error at metallicities below $[\text{Fe}/\text{H}] \sim -1$.

Although the first two possibilities cannot be excluded, we favour the latter option since values of $m_{\text{u}}^{\text{SNII}} \sim 30 M_{\odot}$ are suggested by recent models accounting for metallicity dependent yields of SNII in full detail (e.g. Timmes et al. 1995). We emphasize that the detailed yields for SNII at metallicities $[\text{Fe}/\text{H}] \lesssim -1$ are not important for the sequential enrichment and infall model results for disk stars presented in this paper but we just want to note here that it is difficult to explain the mean $[\text{O}/\text{Fe}]$ ratio in halo stars using the same models.

The observed breakpoint in the $[\text{O}/\text{Fe}]$ vs. $[\text{Fe}/\text{H}]$ relation at $[\text{Fe}/\text{H}] \sim -1.0 \pm 0.2$ (e.g. King 1994) is generally associated with the time SNIa start to contaminate the global disk ISM (e.g. Gilmore & Wyse 1991; Bravo et al. 1993; Ishimaru & Arimoto 1995). In our models, the breakpoint in the $[\text{O}/\text{Fe}]$ vs. $[\text{Fe}/\text{H}]$ relation is mainly determined by: 1) the assumed fraction $\phi^{\text{SNIa}} = 0.005$ of main-sequence stars with initial masses between 2.5 and 8 M_{\odot} (e.g. Nomoto et al. 1984), 2) the delay time $\tau^{\text{SNIa}} = 2.5$ Gyr after which SNIa start to contribute to the enrichment of the ISM (e.g. Smecker-Hane & Wyse 1992; Ishimaru & Arimoto 1995), and 3) the frequency distribution

of SNIa as a function of age for a given stellar generation (assumed to be constant from τ^{SNIa} to $\tau^{\text{SNIa}} + 0.5$ Gyr, and zero otherwise). These assumptions, in particular for τ^{SNIa} , strongly affect the increase of $[\text{Fe}/\text{H}]$ with disk age and thus determine the scatter in and the slope of the $[\text{O}/\text{H}]$ vs. $[\text{Fe}/\text{H}]$ relation predicted. In fact, SNIa provide a background signal of iron-group elements on top of which stellar abundance variations due to sequential enrichment by SNII+SNIb/c occur.

We assumed $\tau^{\text{SNIa}} = 2.5$ Gyr for the models presented in this paper, as recently suggested by Ishimaru & Arimoto (1995). However, this assumption implies different breakpoints in the $[\text{O}/\text{Fe}]$ vs. $[\text{Fe}/\text{H}]$ relation for models with distinct star formation and infall histories. The model shown in Fig. 7-1 predicts $[\text{Fe}/\text{H}] = -1$ after ~ 1.3 Gyr (and results $[\text{Fe}/\text{H}] \sim -0.75$ after 2.5 Gyr). This may indicate that the assumed value of $\tau^{\text{SNIa}} = 2.5$ Gyr is in error. Estimates for τ^{SNIa} based on stellar evolution calculations suffer from large uncertainties in the detailed evolution scenario for SNIa progenitors (see e.g. Smecker-Hane & Wyse 1992; King 1994) while theoretical estimates for τ^{SNIa} based on the observed breakpoint may suffer from large uncertainties in the assumed chemical evolution of the halo (e.g. Ishimaru & Arimoto 1995).

Alternatively, model assumptions related to: 1) the enrichment rate of the disk ISM by SNII (e.g. IMF and SFR, $m_{\text{u}}^{\text{SNII}}$ and SNII yields), or 2) the initial abundances of the material to which the SNII ejecta are mixed (e.g. disk mass at the onset of star formation, amount of gas infall, and infall abundances) may be in error. For instance, adopted iron yields for SNII at metallicities $[\text{Fe}/\text{H}] \lesssim -1$ may be too high by about a factor of two. This would be consistent with the discrepancy in the $[\text{O}/\text{Fe}]$ ratio for Galactic halo stars discussed above. Furthermore, large amounts of metal-poor gas infall would improve the consistency with the assumption of $\tau^{\text{SNIa}} = 2.5$ Gyr. Other possibilities, such as higher values of the disk total-to-final mass-ratio or larger SFR decay times t_{decr} , seem to be excluded by the observations (e.g. van den Hoek et al. 1996).

We conclude that combined sequential enrichment and metal-poor gas infall models are consistent with the observed plateau value and breakpoint in the $[\text{O}/\text{Fe}]$ vs. $[\text{Fe}/\text{H}]$ relation provided that e.g. the adopted SNII yields at low metallicities $[\text{Fe}/\text{H}] \lesssim -1$ are too high by about a factor of two. At the same time, we have illustrated how sensitive our model results are to specific assumptions related to the enrichment by e.g. SNII and SNIa. These assumptions may affect quantitative conclusions concerning the relative importance of sequential stellar enrichment and metal-poor gas infall. However, our qualitative conclusion regarding the simultaneous presence of these processes in the local Galactic disk is not altered.

5.2. Observational support and implications for Galactic chemical evolution

We briefly discuss observational evidence in support of sequential stellar enrichment and metal-deficient gas infall in the local disk ISM, and consider possible implications for the chemical evolution of the Galaxy as a whole.

Sequential star formation has been argued to occur in nearby molecular cloud complexes including the well known Orion, Taurus-Auriga-Perseus, Cepheus, Carina, and Chameleon cloud complexes (e.g. see the review by Blaauw 1991; Megeath et al. 1995; Testi et al. 1995; Goldsmith 1995). In the Orion molecular cloud complex, age differences between OB subgroups are typically $\sim 2-7$ Myr (e.g. Genzel & Stutzki 1989; Cunha & Lambert 1992). When star formation proceeds on such time scales, massive stars belonging to different OB subgroups may enrich the ambient molecular cloud material before a next round of star formation is initiated. Interestingly, the oldest OB subgroups in the Orion OB1 association appear to have oxygen abundances that are lower by about 40% (~ 0.2 dex in $[\text{O}/\text{H}]$) compared to the younger subgroups (see e.g. Olive & Schramm 1982; Cunha & Lambert 1992).

Apart from observational support for sequential enrichment in nearby star forming regions, there are strong indications that the molecular cloud out of which the Sun formed has been enriched sequentially as well. Studies related to extinct radioactive nuclides such as ^{53}Mn both in the Sun and in meteorites suggest that the protosolar molecular cloud has been enriched by high mass stars from a preceding OB association, about 10–25 Myr prior to the actual formation of the Sun (e.g. Cameron 1993; Swindle 1993).

Observations suggest that high-velocity inflow of metal-deficient gas towards the Galactic disk is a common phenomenon as well (e.g. de Boer & Savage 1984; Wakker 1990; Schwarz et al. 1995). Estimates of the current gas infall rate onto the Galactic disk range from 0.2–0.5 $M_{\odot} \text{ yr}^{-1}$, based on high-velocity clouds (HVCs; $v \gtrsim 250 \text{ km s}^{-1}$; e.g. Mirabel & Morras 1984; Lépine & Duvert 1994), to $\sim 0.7 M_{\odot} \text{ yr}^{-1}$ derived from the soft X-ray background (Cox & Smith 1976), and $\sim 1.5 M_{\odot} \text{ yr}^{-1}$ based on observations of atomic hydrogen (Oort 1970). Since gas infall rates derived from the inflow of HVCs are likely underestimates (e.g. Mirabel & Morras 1984), we estimate that $\sim 30-40$ % of the stars currently forming in the Galactic disk may be associated with infall (assuming a current SFR of $\sim 3.5 M_{\odot} \text{ yr}^{-1}$; e.g. Dopita 1987).

Observational support for infall induced star formation in the SNBH has recently been presented for the Orion cloud complex (Lépine & Duvert 1994; Meyer et al. 1994), the Gould Belt (e.g. C  meron & Torra 1994), and the ζ Sculptoris open cluster (Edvardsson et al. 1995). These observations suggest that the most prominent star forming regions in the SNBH have been partly formed from infalling clouds from the Galactic halo. Circumstantial ev-

idence for HVC impacts on the Galactic disk is based on: 1) the existence of subgroups of young stars in star forming molecular clouds at high Galactic latitudes (like the Orion molecular cloud complex), 2) the displacement of OB star clusters with respect to the centers of their parent molecular clouds, 3) the alignment of the OB clusters in directions that are substantially inclined to the Galactic plane, 4) the age sequence of the aligned OB associations with an age of $\sim 10^7$ yr for the oldest subgroups, and 5) the large elongated or filamentary structures observed in e.g. the Orion, Taurus, Monoceros molecular clouds connecting the clouds to the Galactic plane (see also Tenorio-Tagle et al. 1986; Franco et al. 1988; G  mez de Castro 1992). Many of these phenomena can be naturally explained by the interaction of a high velocity cloud with disk ISM and are difficult to reproduce by the process of sequential star formation (L  pine & Duvert 1994). Consequently, infall induced star formation appears to be a process frequently operating in the Galactic disk.

We have argued that metal-deficient gas infall and sequential stellar enrichment are likely to play an important role for the inhomogeneous chemical evolution of the Galactic disk. These processes probably occur on scales ranging from single molecular clouds to the formation sites of open and globular clusters (e.g. Brown 1991). Large abundance variations of ~ 0.3 dex in $[\text{O}/\text{Fe}]$ observed among metal-poor halo stars (e.g. Bessell et al. 1991; Nissen et al. 1994) suggest that sequential enrichment and gas accretion have been important for the chemical evolution of the Galactic halo as well.

Nevertheless, combined metal-poor gas infall and sequential stellar enrichment may be a too schematic picture of the complex set of processes directing the chemical evolution of the Galactic disk. In particular, merger events with small companion galaxies may be important as well (e.g. Quinn et al. 1993). In such case, both gas and stars in the companion galaxy may add substantially to the observed abundance inhomogeneities in the Galactic disk (Pilyugin & Edmunds 1995b). However, the suggestion that stellar populations from merging companion galaxies contribute substantially to the observed stellar abundance variations in the Galactic disk seems difficult to reconcile with: 1) the apparent homogeneous distribution of these variations within the metallicity range observed at a given age of the disk, and 2) the small scatter observed in the element-to-element variations for stars in the SNBH. Notwithstanding, merging may be important for the chemical evolution of the Galaxy by adding large amounts of predominantly metal-poor material and initiating star formation in the disk.

Inhomogeneous chemical evolution due to sequential stellar enrichment and/or metal-poor gas infall is probably important also in nearby galaxies such as the Magellanic Clouds and M31. In the Large Magellanic Cloud, large abundance variations of $\sim 0.4-0.8$ dex in $[\text{Fe}/\text{H}]$ among similarly aged open clusters are observed (e.g. Cohen et

al. 1982; Da Costa 1991; Olsewski et al. 1991). Part of the variations may be accounted for by a radial gradient of ~ 0.15 dex kpc^{-1} in $[\text{Fe}/\text{H}]$ (Kontizas et al. 1993). However, the main part of these variations is likely due to triggered star formation in supershells as indicated by the close association of HII complexes with large HI holes observed in the LMC (Dopita 1985; Lortet & Testor 1988). In addition, gas infall may have affected the chemical evolution of the tidally interacting Magellanic Clouds.

Observational evidence in support of shock-induced star formation by SNII in the spiral arms of M31 has been presented by Magnier et al. (1992). At these sites, young OB stars are observed to initiate recent star formation so that large abundance inhomogeneities due to sequential stellar enrichment are expected, similar to those observed among OB associations in the Orion star forming cloud complex in our own Galaxy.

Stellar and nebular abundance indicators reveal that substantial abundance fluctuations exist in the ISM of gas-rich galaxies (e.g. Roy & Kunth 1995). For instance, abundance inhomogeneities in metal-poor galaxies such as IZw 18 may be among the largest observed in external galaxies (e.g. Kunth et al. 1995) although this is still highly uncertain (Pettini & Lipman 1995). Whether the abundance fluctuations observed in dwarf galaxies are due to variations in self-enrichment of the HII-regions in these systems (e.g. Pilyugin 1992) and/or are related to selective loss of metals through galactic winds driven by massive stars (Roy & Kunth 1995; Martin 1996) is unclear.

We expect that sequential stellar enrichment is generally inefficient in dwarf galaxies because of their low gas densities, and that the effect of metal-poor gas infall on the stellar abundance variations is weak due to their low ISM abundances. Instead, star formation and abundance inhomogeneities induced by *metal-rich* gas infall may be relatively important in these systems.

Acknowledgements. It is a pleasure to thank L.S. Pilyugin, K. Nomoto, and J.-R. Roy for stimulating discussions. We like to thank J. van Paradijs for a critical reading of earlier versions of this paper. We are grateful to the referee, Dr. B. Pagel, for careful and constructive remarks from which this paper has benefitted. The research of LBH is supported under grant 782-372-028 by the Netherlands Foundation for Research in Astronomy (ASTRON), which is financially supported by the Netherlands Organisation for Scientific Research (NWO).

A. Appendix

We describe the adopted model for the inhomogeneous chemical evolution of a star forming gas cloud. The model can be applied to various mass scales, e.g. to the entire system of molecular cloud complexes in the Galactic disk or to the star forming core regions within a single molecular cloud. We start from a homogeneous, metal free gas cloud with a total mass

M_{cl} . At any evolution time t in its evolution, this cloud is subdivided into N_{scl} active subclouds (with corresponding masses M_{scl}^i) involved with star formation and an inactive cloud part (with mass M_{qcl}) not involved with star formation. We assume matter to be freely exchanged within the inactive cloud part. Each subcloud i is formed at corresponding evolution times t_{scl}^i and is allowed to follow its individual star formation, mixing, and infall history.

A.1. Model description, definitions and assumptions

During the lifetime t_{ev} of the star forming gas cloud a total number N_{sf} star formation events is assumed occur. Each star formation event j presumably occurs within an active subcloud i . We define N_{sf}^i as the total number of star formation events within subcloud i . For the reference model $N_{\text{sf}}^i = 1$ and each star formation event j occurs in corresponding subcloud $i = j$. Subclouds are allowed to experience numerous star formation events, i.e. $N_{\text{sf}} > 1$. During each star formation event j at time $t = t_{\text{sf}}^j$ within subcloud i , a total mass of gas $\delta M_{\text{scl}}^i = \epsilon^j M_{\text{scl}}^i(t_{\text{sf}}^j)$ is transformed into stars.

We define Δt_{disp}^j as the time between the onset of star formation within a subcloud core and the complete dispersal of this core region by supernova explosions and/or stellar winds. During Δt_{disp}^j the subcloud core is assumed to form stars. The profile of the star formation rate (SFR) during Δt_{disp}^j is assumed constant and identical for all star formation events. However, quantities such as the minimum stellar mass formed and IMF-slope are allowed to vary from one star formation event to another (cf. Sect. 4.2). The subcloud core dispersal time determines the mass of the most massive star that is able to enrich subcloud cloud material before the core ultimately breaks up. At time of core dispersal, the newly formed generation of stars has returned an amount of material δM_{ret}^j . Accordingly, the *net* amount of material converted into stars during star formation event j is given by: $\delta M_{\text{sf}}^j = \epsilon^j \delta M_{\text{scl}}^i(t_{\text{sf}}^j) - \delta M_{\text{ret}}^j$.

Subclouds M_{scl}^i are formed from the inactive cloud ISM at cloud evolution times $t = t_{\text{scl}}^i$. When a subcloud forms it adopts the abundances of the inactive cloud ISM at $t = t_{\text{scl}}^i$. For each subcloud, we define a mixing time scale Δt_{mix}^i as the time between formation of the subcloud and the actual break up of the entire subcloud. The instant of break up of the subcloud may be either after one or more star formation events, or before star formation actually takes place. In this manner, material can be deposited within a subcloud region for a considerable period of time before being mixed to the surrounding ISM. The mixing history of each subcloud directs both the inhomogeneous chemical evolution of the inactive cloud and that of the neighboring subclouds.

Before an entire subcloud breaks up its constituent material will be enriched by the stellar populations it is hosting. We assume the stellar enrichment of the subcloud to proceed homogeneously. In order to allow for sequential enrichment, we consider a fraction λ^j of enriched material ejected *during* star formation event j to mix homogeneously with subcloud core material hosting the *next* star formation event. Simultaneous with the ejection of enriched material returned by newly formed stars, a substantial fraction of the ambient subcloud matter $\kappa^j M_{\text{scl}}^i$ may be swept up during dispersal of its star forming core. This subcloud material may mix to the subcloud hosting the next star formation event as well. The subcloud

hosting the next star formation event may be either the subcloud hosting the current star formation event or a subcloud nearby. No matter exchange is assumed between the subcloud and the surrounding ISM during the time between two star formation events occurring within one and the same subcloud. In case of the reference model, we do not consider mass transfer between subclouds, i.e. $\lambda^j = \kappa^j = 0$.

After an entire subcloud breaks up its matter is assumed to mix homogeneously to the inactive cloud part. At the same time, stars associated with the dispersing subcloud become part of the stellar populations in the inactive cloud. After break up, different cloud fragments present in the ambient ISM may form new subclouds wherein star formation occurs as soon as the critical conditions for star formation are met.

In addition to the individual chemical evolution of subclouds, which is directed by their star formation history and exchange history with the surrounding ISM, we allow for local enrichment of a given subcloud by stars that were *not* formed within that subcloud. This may be particularly important for low mass SNIa-progenitors which travelled considerable distances from their birth sites and enrich their immediate surroundings at the time they explode as SNIa (cf. Fig. 2f; see below).

A.2. Basic equations

We keep track of the total mass of and abundances in stars and gas as a function of evolution time, both within each subcloud and the inactive cloud ISM. For each star formation event we use conventional chemical evolution model equations (e.g. Tinsley 1980, see below) except for including metallicity dependent stellar lifetimes, remnant masses and element yields (cf. van den Hoek et al. 1996).

A.2.1. Mass-exchange between subclouds and the inactive cloud ISM

We denote ΔQ as the variation of a quantity Q between two cloud evolution times $t - \Delta t$ and t . With $M_{\text{cl}}(t = 0)$ the initial mass of the cloud and no stars initially present, i.e. $M_*(0) = 0$, we can express the variations of mass of gas and stars within the cloud as:

$$\Delta M_{\text{cl}} = \sum_{i=1}^{N_{\text{scl}}(t)} \Delta M_{\text{scl}}^i + \Delta M_{\text{qcl}} \quad (\text{A1})$$

$$\Delta M_* = \sum_{j=1}^{N_{\text{sf}}(t)} (\Delta C_*^j - \Delta E_*^j) - \Delta E_{*,\text{qcl}} \quad (\text{A2})$$

where $N_{\text{scl}}(t)$ is the current number of individual subclouds, $N_{\text{sf}}(t)$ the current number of star formation events within the cloud, ΔC_*^j the total mass of stars formed during star formation event j , and ΔE_*^j the total mass of matter returned within Δt by stars formed during star formation event j . We recall conventional expressions for ΔC_*^j and ΔE_*^j (cf. Tinsley 1980):

$$\Delta C_*^j = \int_{t_{\text{sf}}}^{t_{\text{sf}} + t_{\text{disp}}} \int_{m_1}^{m_u} m S_j(t) M_j(m) dm dt \quad (\text{A3})$$

$$\Delta E_*^j = \int_{t - \Delta t}^t \int_{m_o(t - t_{\text{sf}})}^{m_o(t - t_{\text{sf}} - t_{\text{disp}})} (m - m_{\text{rem}}(m)) S_j(t - \tau(m)) M_j(m) dm dt \quad (\text{A4})$$

where S_j and M_j denote the SFR by number [yr^{-1}] and IMF [M_{\odot}^{-1}] for star formation event j . For convenience, we ignored the index j for t_{sf} , t_{disp} as well as for the stellar mass

boundaries at birth m_l , m_u . We emphasize that both the stellar remnant masses $m_{\text{rem}}(m)$, lifetimes $\tau(m)$, and turnoff-masses $m_o(t)$ are a function of the initial metallicity Z_* (containing all elements heavier than He) of the stellar generation under consideration. Variations in the total gas masses within the inactive cloud and subcloud i , i.e. M_{qcl} and M_{scl}^i respectively, can be expressed as:

$$\Delta M_{\text{qcl}} = \Delta E_{*,\text{qcl}} - \Sigma_{\text{form}} M_{\text{scl}}^k + \Sigma_{\text{disp}} M_{\text{scl}}^l \quad (\text{A5})$$

$$\Delta M_{\text{scl}}^i = [\Delta E_* - \Delta C_*]^i + \Delta M_{\text{sf,prev}} - \Delta M_{\text{sf,next}} \quad (\text{A6})$$

$$\Delta M_{\text{scl}} = \sum_{i=1}^{N_{\text{scl}}(t)} \Delta M_{\text{scl}}^i + \Sigma_{\text{form}} M_{\text{scl}}^k - \Sigma_{\text{disp}} M_{\text{scl}}^l \quad (\text{A7})$$

where $\Delta E_{*,\text{qcl}}$ refers to the amount of material returned by stars present in the inactive cloud within time Δt . We followed both the stellar ejecta from recently formed stars within active subclouds and the ejecta from older stellar populations present in the inactive cloud ISM. The total amount of gas depleted by subclouds which are formed within time Δt is denoted by $\Sigma_{\text{form}} M_{\text{scl}}^k$. Similarly, the amount of gas returned by subclouds which become dispersed within time Δt is denoted by $\Sigma_{\text{disp}} M_{\text{scl}}^l$. We remark that the term between square brackets in Eq. (A6) refers to star formation events which occur *within* subcloud i .

A.2.2. Supernovae Type Ia

The term ΔE_*^i in Eq. (A6) is related both to stellar generations which formed within subcloud i and to stars that entered the subcloud from elsewhere in the cloud. We will consider the case of SNIa progenitors stars only. Consequently, the term ΔE_*^i can be expressed as two terms, i.e. $\Delta E_*^i = \Sigma_{\text{sf}} (\Delta E_*^j)^i_{\text{scl}} + \Delta E_{\text{SNIa}}$. The former term is related to star formation events which occurred within subcloud i while the latter term is associated with subcloud enrichment by SNIa-progenitors formed elsewhere in the cloud. We define the total amount of matter returned by SNIa within subcloud i during time Δt as: $\Delta E_{\text{SNIa}} \equiv \alpha_{\text{SNIa}}^i \Delta t R_{\text{SNIa}} m_{\text{rem}}(m)$ where R_{SNIa} is the total average SNIa-rate in the entire cloud and α_{SNIa}^i the corresponding fraction of SNIa that is assumed to go off within subcloud i . In case of the reference model $\Delta E_{\text{SNIa}} = 0$.

A.2.3. Mass-exchange between individual subclouds

As matter may be transferred from one subcloud to another (or within one subcloud from one subcloud core to another) we include terms $\Delta M_{\text{sf,prev}}$ and $\Delta M_{\text{sf,next}}$ in Eq. (A6). The term $\Delta M_{\text{sf,prev}}$ corresponds to the amount of material added from the *preceding* star formation event to the core of the subcloud currently experiencing star formation. The term $\Delta M_{\text{sf,next}}$ refers to the amount of matter mixed from the subcloud core actually experiencing star formation to the subcloud core hosting the *next* star formation event. For each star formation event j which happens to occur in subcloud i within the time interval Δt we may write:

$$\Delta M_{\text{sf,prev}} = \lambda^{j-1} \delta M_{\text{ret}}^{j-1} + \kappa^{j-1} M_{\text{scl,prev}} \quad (\text{A8})$$

$$\Delta M_{\text{sf,next}} = \lambda^j \delta M_{\text{ret}}^j + \kappa^j M_{\text{scl}}^i \quad (\text{A9})$$

where $M_{\text{scl,prev}}$ is the mass of the subcloud hosting the preceding star formation event. In this paper, we presented only results for $\kappa^j = 0$. In general, $\kappa^j > 0$ has a similar effect as when reducing the sequential enrichment efficiency λ^j .

A.2.4. Chemical evolution of subclouds and inactive cloud ISM

Expressions for the average abundance changes of element X within the entire cloud, inactive cloud part, and subclouds can be written as:

$$\Delta(X_{\text{cl}}M_{\text{cl}}) = \sum_{i=1}^{N_{\text{scl}}(t)} \Delta(X_{\text{scl}}^i M_{\text{scl}}^i) + \Delta(X_{\text{qcl}}M_{\text{qcl}}) \quad (\text{A10})$$

$$\Delta(X_{\text{qcl}}M_{\text{qcl}}) = \Delta E_{X,\text{qcl}} - \Sigma_{\text{form}} X_{\text{qcl}} M_{\text{scl}}^k + \Sigma_{\text{disp}} X_{\text{sf}}^l (M_{\text{scl}}^l) \quad (\text{A11})$$

$$\Delta(X_{\text{scl}}M_{\text{scl}}) =$$

$$\sum_{i=1}^{N_{\text{scl}}(t)} \Delta(X_{\text{scl}}^i M_{\text{scl}}^i) + \Sigma_{\text{form}} X_{\text{qcl}} M_{\text{scl}}^k - \Sigma_{\text{disp}} X_{\text{sf}}^l M_{\text{scl}}^l \quad (\text{A12})$$

$$\Delta(X_{\text{scl}}^i M_{\text{cl}}^i) = [\Delta E_X - X_{\text{scl}} \Delta C_*]^i \Delta M_{X,\text{pre}} - \Delta M_{X,\text{next}} \quad (\text{A13})$$

where the meaning of each term can be found from its counterpart in Eqs. A5-A7. Similarly, expressions for $\Delta M_{X,\text{prev}}$ and $\Delta M_{X,\text{next}}$ can be written as:

$$\Delta M_{X,\text{prev}} = \lambda^{j-1} \delta M_{X,\text{ret}}^{j-1} + \kappa^{j-1} (X_{\text{scl}} M_{\text{scl}})_{\text{prev}} \quad (\text{A14})$$

$$\Delta M_{X,\text{next}} = \lambda^j \delta M_{X,\text{ret}}^j + \kappa^j X_{\text{scl}}^i M_{\text{scl}}^i \quad (\text{A15})$$

where ΔE_X^j is the total mass of enriched material of element X returned within time Δt by a stellar generation formed during star formation event j :

$$\Delta E_X^j = \int_{t-\Delta t}^t \int_{m_o(t-t_{\text{sf}})}^{m_o(t-t_{\text{dis}})} \Delta M_X(m) S_j(t-\tau(m)) M_j(m) dm dt \quad (\text{A16})$$

$$\Delta M_X(m) = mp_X(m) + (m - m_{\text{rem}}(m)) X_*^j \quad (\text{A17})$$

and $\Delta M_X(m)$ is the total mass of element X ejected by a star of initial mass m born with metallicity X_*^j during star formation event j . The term $\Delta M_X(m)$ includes both newly synthesized stellar material and matter initially present at the time stars were formed. Initial stellar abundances X_*^j are determined by the abundances of the subcloud i (hosting star formation event j) at time t_{sf}^j , i.e. $X_*^j = X_{\text{scl}}^i(t = t_{\text{sf}}^j)$. Literature sources for the adopted theoretical metallicity dependent stellar yields $p_X(m)$, stellar lifetimes $\tau(m)$, and remnant masses $m_{\text{rem}}(m)$ are given in Sect. 3.4.

References

- Anders E. & Grevesse N. 1989, *Geochim. Cosmochim. Acta* 53, 197
- Andersson H. & Edvardsson B. 1995, *A&A* 290, 590
- Baldwin J.A., Ferland G., Martin P.G., et al. 1991, *ApJ* 374, 580
- Bahcall J.N. & Pinsonneault M.H. 1995, to appear in: *Review of Modern Physics*
- Bahcall J.N. & Soneira R.M. 1980, *ApJS* 44, 73
- Basu S. & Rana N.C. 1992, *Ap&SS* 196, 1
- Bateman N.P.T. & Larson R.B. 1993, *ApJ* 407, 634
- van den Bergh S. & Tammann G.A. 1991, *ARA&A* 29, p. 363
- Bessell M.S., Sutherland R.S., Ruan K. 1991, *ApJ* 383, L71
- Binney J. & Tremaine S. 1987, *Galactic Dynamics*, Princeton Univ. Press, Princeton
- de Boer K.S. & Savage B.D. 1984, *A&A* 136, L7
- Blaauw A. 1991, in: Lada J., Kylafis N.D. (eds.) *The Physics of Star Formation and Early Stellar Evolution*, NATO ASI Series
- Boesgaard A.M. 1989, *ApJ* 336, 798
- Bravo E., Isern J., Canal R. 1993, *A&A* 270, 288
- Brown J.H. 1991, Ph.D. Thesis, Univ. of Illinois, Urbana-Champaign.
- Buonanno R., Corsi C.E., Fusi Pecci F. 1989, *A&A* 216, 80
- Cameron A.G.W. 1993, in: Levy E.H., Lunine J.I. (eds.) *Protostars and Planets III*, Univ. of Arizona Press, p. 43
- Capellaro E., Turatto H, Benetti S., et al. . 1993, *A&A* 273, 383
- Carlberg R.G., Dawson P.C., Hsu T., van den Berg D.A. 1985, *ApJ* 294, 674
- Carney B.W., Latham D.W., Laird J.B. 1990, *AJ* 99, 752
- Carraro G. & Chiosi C. 1994, *A&A* 287, 761
- Cioffi D.F. & Shull J.M. 1991, *ApJ* 367, 96
- Clayton D.D. 1988, *MNRAS* 234, 1
- Cohen J.G. 1982, *ApJ* 258, 143
- Cómeron F. & Torra J. 1994, *A&A* 281, 35
- Cox D.P. & Smith B.W. 1974, *ApJ* 189, L105
- Cunha K., & Lambert D.L. 1992, *ApJ* 399, 586
- Da Costa G.S. 1991, in: Haynes R.F., Milne D.G. (eds.) *The Magellanic Clouds and their Dynamical Interaction with the Milky Way*, IAU Symp. 148, Kluwer, Dordrecht, p. 183
- Dopita M.A. 1985, *ApJ* 295, L5
- Dopita M.A. 1987, in: Faber S.M. (ed.) *Nearly Normal Galaxies from the Planck Time to Present*, Springer, New York, p. 144
- Dopita M.A. 1990, in: Thronson H.A., Shull J.M. (eds.) *The Interstellar Medium in Galaxies*, Kluwer, Dordrecht, p. 437
- Edmunds M.G. 1975, *Ap&SS* 32, 483
- Edmunds M.G., 1993 *Nat* 365, 293
- Edvardsson B., Andersen J., Gustafsson B., et al. 1993a, *A&A* 275, 101 (**EDV**)
- Edvardsson B., Andersen J., Gustafsson B., et al. 1993b, *A&AS* 102, 603
- Edvardsson B., Petterson B., Kharrazi M., Westerlund B. 1995, *A&A* 293, 75
- Elmegreen B.G. & Lada C.J. 1977, *ApJ* 214, 725
- Fich M. & Tremaine S. 1991, *ARA&A* 29, 409
- Fitzsimmons A., Brown P.J.F., Dufton P.L., and Lennon D.J. 1990, *A&A* 250, 159 de Freitas Pacheco J.A. 1993, *ApJ* 403, 673
- Franco J., Tenorio-Tagle G., Bodenheimer P., Rózycka M., Mirabel I.F., 1988, *ApJ* 333, 826
- Franco P., & Matteucci F. 1993, 280, 136
- Friel E.D. & Janes K.A. 1993, *A&A* 267, 75
- García-Lopez et al. 1993, *ApJ* 412, 173
- Garmany C.D., Conti P.S., Chiosi C., 1982, *ApJ* 263, 777
- Gehren T., Nissen P.E., Kudritzki R.P., Butler K. 1985, in: Danziger I.J., Matteucci F., Kjaer K. (eds.) *Abundance Gradients in the Galactic Disk from young B-type Stars in Clusters*, ESO Conf. and Workshop Proc. 21, p. 171
- Genzel R. & Stutzki J. 1989, *ARA&A* 27, 41
- Gies D.R., and Lambert D.L. 1992, *ApJ* 387, 673
- Gilmore G. 1989, in: Buser R., King I.R. (eds.) *The Milky Way as a Galaxy*, Univ. Science Books, Mill Valley Ca., p. 281
- Gilmore G., & Wyse R.F.G. 1991, *ApJ* 367, L55
- Goldsmith P.F. 1995, to appear in: Chiao R.Y. (ed.) *C.H. Townes Festschrift*, Arcibo preprint
- Gómez de Castro A.I. 1992, in: Palous J., Burton W.B., Lindblad P.O (eds.) *Evolution of the Interstellar Medium and Dynamics of Galaxies*, Cambridge Univ. Press
- Gratton R.G. & Sneden C. 1991, *A&A* 241, 501
- Grenon M. 1987, *JA&A* 8, 3
- Grenon M. 1989, *Ap&SS* 156, 29
- Grevesse N. & Noels A. 1993, *Phys. Scripta* T47, 133
- Groenewegen M.A.T. & de Jong T. 1993, *A&A* 267, 410
- Groenewegen M.A.T., van den Hoek L.B., de Jong T., 1995, *A&A* 293, 381
- Haikala L.K. 1995, *A&A* 294, 89

- Hashimoto M., Iwamoto K., Nomoto K. 1993, *ApJ* 414, L105
 Hashimoto M., Nomoto K., Tsujimoto T., Thielemann F.-K. 1993, in: Käppeler F., Wisshak K. (eds.) *Nuclei in Cosmos*, Institute Physics Publ., p. 587
 Henning T. & Gürtler J. 1986, *Ap&SS* 128, 199
 van den Hoek L.B., Groenewegen M.A.T., Nomoto K., and de Jong T. 1996, *A&A in preparation*
 Ishimaru Y. & Arimoto N. 1995, *A&A*, *submitted*
 Kaufer A., Szeifert Th., Krenzlin R., Baschek B., Wolf B. 1994, *A&A* 289, 740
 Kennicutt R.C., Jr. 1983, *ApJ* 272, 54
 King J.R. 1994, *AJ* 107, 350
 King D.L., Vladilo G., Lipman K., et al. 1995, to appear in *A&A*
 Klochkova V.G., Mishenina T.V. & Panchuk V.E. 1989, *Soviet Astron. Lett.* 15, 135
 Kontizas M., Kontizas E., Michalitsianos A.G. 1993, *A&A* 269, 107
 Kulkarni S.R. & Heiles C. 1987, in: Hollenbach D.J., Thronson H.A. (eds.) *Interstellar Processes*, Reidel, Dordrecht, p. 87
 Kunth D., Lequeux J., Sargent W.L.W., Viallefond F. 1994, *A&A* 282, 709
 Kunth D., Matteucci F., Marconi G. 1995, *A&A* 297, 634
 Lambert D.L. 1989, in: Waddington C.J. (ed.) *Cosmic Abundances of Matter*, Amer. Inst. Phys., New York, p. 168
 Larson R.B. 1969, *MNRAS* 145, 504
 Larson R.B. 1976, *MNRAS* 176, 31
 Larson R.B., Tinsley B.M., Caldwell C.N. 1980, *AJ* 237, 692
 Lennon D.J., Dufton P.L., Fitzsimmons A., Gehren T., Nissen P.E. 1990, *A&A* 240, 349
 Leisawitz D.T. 1985, Ph.D. Thesis, Univ. of Texas, Austin
 Lépine J.R.D. & Duvert G. 1994, *A&A* 286, 60
 Lortet M.-C. & Testor G. 1988, *A&A* 194, 11
 Maeder A. 1992, *A&A* 264, 105
 Maeder A. 1993, *A&A* 268, 833
 Magnier E.A., Lewin W.H.G., van Paradijs J., et al. 1992, *A&AS* 96, 379
 Martin C.L., 1996, *ApJ*, in press
 Mayor M. 1976, *A&A* 48, 301
 Mayor M. & Martinet L. 1977, *A&A* 55, 221
 Megeath S.T., Cox P., Bronfman L., Roelfsema P.R. 1995, to appear in *A&A*
 Meusinger H., Reimann H.-G., and Stecklum B. 1991, *A&A* 245, 57
 Meyer D.M., Jura M., Hawkins I., Cardelli J.A. 1994, *ApJ* 437, L59
 Mezger P.G. 1988, in: Pudritz R.E., Fich M. (eds.) *Galactic and Extragalactic Star Formation*, Kluwer, Dordrecht, p. 227
 Mirabel I.F. & Morras R. 1984, *ApJ* 279, 86
 Nissen P.E. 1988, *A&A* 199, 46
 Nissen P.E., Gustafsson B., Edvardsson B., Gilmore G., 1994, *A&A* 285, 440
 Nomoto K., Thielemann F.-K., Yokoi K. 1984, *ApJ* 286, 644
 Nomoto K., Kumagai S., Shigeyama T. 1991, in: Durouchoux P., Prantzos P. (eds.) *Gamma-Ray Line Astrophysics*, AIP Conf. Proc. 232, AIP, New York, p. 236
 Nomoto K. et al. 1993, *Nat* 364, 507
 Nomoto K., Iwamoto K., Tsujimoto T., Hashimoto M. 1994, in: Suzuki Y., Nakamura K. (eds.) *Frontiers of Neutrino Olive K.A., & Schramm D.N. 1982, ApJ 257, 276*
 Olsewski E.W., Schommer R.A., Suntzeff N.B., Harris H.C. 1991, *AJ* 101, 515
 Ogelman H.B. & Maran S.P. 1976, *ApJ* 209, 124
 Osterbrock D.E., Tran H.D., Veilleux S. 1992, *ApJ* 389, 305
 Pagel B.E.J. & Tautvaišienė G. 1995, *MNRAS* 276, 505
 Peimbert M. 1987, in: *Star Forming Regions*, Conf. Proc., Tokyo, Reidel, Dordrecht, p. 111
 Peimbert M., Storey P.J., Torres-Peimbert S. 1993, *ApJ* 414, 626
 Pettini M. & Lipman K., 1995, *A&A*, in press
 Pismis 1990, *A&A* 234, 443
 Pilyugin L.S. 1992, *A&A* 260, 58
 Pilyugin L.S. & Edmunds M.G. 1995a, *A&A*, *submitted*
 Pilyugin L.S. & Edmunds M.G. 1995b, in: 'The Interplay between Massive Star Formation, the ISM and Galaxy Evolution', 11th IAP Ap. Meeting, Paris, Kunth D., Guiderdoni B., Heydari-Malayeri M., Thuan T.X., and Van J.T.T. (Eds.)
 Prantzos N. 1994, *A&A* 284, 477
 Quinn P.J., Hernquist L., Fullagar D.P. 1993, *ApJ* 403, 74
 Rizzo J.R. & Bajaja E. 1994, *A&A* 289, 922
 Rolleston W.R.J., Dufton P.L., Fitzsimmons A. 1994, *A&A* 284, 72
 Roy J.-R., & Kunth D. 1995, *A&A* 294, 432
 Schaller G., Schaerer D., Meynet G., Maeder A. 1992, *A&AS* 96, 269
 Schuster W.J., & Nissen P.E. 1989, *A&A* 222, 69
 Schwarz U.J., Wakker B.P., van Woerden H. 1995, *A&A* 302, 364
 Shaver P.A., McGee R.X., Newton L.M., et al. 1983, *MNRAS* 204, 53
 Shigeyama T. et al. 1990, *ApJ* 361, L23
 Smecker-Hane T.A. & Wyse R.F.G. 1992, *AJ* 103, 1621
 Steigman G. 1993, *ApJ* 413, L73
 Strobel A. 1991, *A&A* 247, 35
 Strom R.G. 1993, in NATO ASI Series Vol. 450 on *The lives of Neutron Stars*, Eds. M.A. Alpar, Ü. Kiziloglu, and J. van Paradijs, 23
 Swindle T.D. 1993, in: Levy E.H., Lunine J.I. (eds.) *Protostars and Planets III*, Univ. of Arizona Press, p. 867
 Tenorio-Tagle G., Bodenheimer P., Różyczka M., Franco J. 1986, *A&A* 170, 107
 Testi L., Olmi L., Hunt L., et al. 1995, to appear in *A&A*
 Thielemann F.-K., Nomoto K., Hashimoto M. 1994, in: Audouze J., Bludman S., Mochkovitz R., Zinn-Justin J. (eds.) *Supernovae*, Proc. Session LIV, Les Houches, Elsevier Sci. Publ. Amsterdam, p. 629
 Thuan T.X., et al. 1995, *A&A*, *in preparation*
 Timmes F.X., Woosley S.E., Weaver T.A. 1995, *ApJS* 98, 617
 Tinsley B.M. 1980, *Fund. Cosmic Phys.* 5, 287
 Trimble V. 1991, *A&AR* 3, 1
 Tsujimoto T., Nomoto K., Hashimoto M., Thielemann F.-K. 1995, *submitted to ApJ*
 Tutukov V.A., Yungelson L.R., Iben I., Jr. 1992, *ApJ* 386, 197
 Twarog B.A. 1980a, *ApJ* 242, 242
 Twarog B.A. 1980b, *ApJS* 44, 1
 Twarog B.A. & Wheeler J.C. 1982, *ApJ* 261, 636
 Wakker B.P. 1990, Ph.D. Thesis, Univ. of Groningen
 Walterbos R.A.M. 1988, in: Pudritz R.E., Fich M. (eds.) *Galactic and Extragalactic Star Formation*, NATI/ASI Conf. Proc. 232, p. 361
 Wielen R., Fuchs B., Dettbarn C., 1996, *A&A*, in press
 Wilking B.A. & Lada C.J. 1983, *ApJ* 274, 571
 Wilmes M. & Köppen J. 1995, *A&A* 294, 47
 Wilson T.L. & Matteucci F. 1992, *A&AR* 4, 141
 Woosley S.E., Langer N., Weaver T.A. 1993, *ApJ* 411, 823
 Woosley S.E., Langer N., Weaver T.A. 1995, *ApJ* 448, 315
 Yamaoka H. 1993, Ph.D. Thesis, Univ. of Tokyo
 York D.G., Spitzer L., Bohlin R.C., et al. 1983, *ApJ* 266, L55